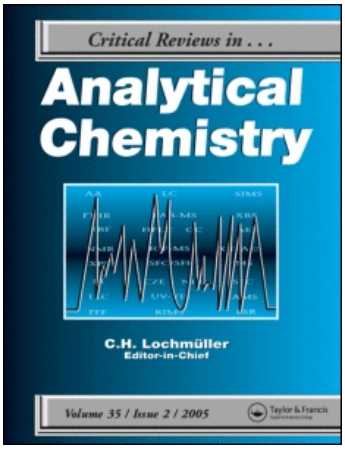

Critical Reviews in Analytical Chemistry
Publication details, including instructions for authors and subscription information:
http://www.informaworld.com/smpp/title~content=t713400837

Luminescence of Micellar Solutions

Ray von Wandruszka[a]
[a] Department of Chemistry, University of Idaho, Moscow, ID

To cite this Article von Wandruszka, Ray(1992) 'Luminescence of Micellar Solutions', Critical Reviews in Analytical Chemistry, 23: 3, 187 — 215
To link to this Article: DOI: 10.1080/10408349208050854
URL: http://dx.doi.org/10.1080/10408349208050854

Critical Reviews in Analytical Chemistry, 23(3):187–215 (1992)

Luminescence of Micellar Solutions

Ray von Wandruszka
Department of Chemistry, University of Idaho, Moscow, ID 83843

ABSTRACT: Luminescence spectroscopy provides a unique set of tools for the study of micellar systems. Variations in emission and excitation spectra of fluorescent probes may be used to assess the onset of micellization, while fluorescence lifetime, anisotropy, sensitization, and quenching measurements have made it possible to determine important micellar characteristics. Thus, critical micelle concentrations; micellar aggregation numbers; shapes, sizes, and structures of micelles; and micellar microviscosities have been determined. Work has been carried out with both normal and reverse micelles, and the influence of various solution-borne species on these aggregates has been evaluated through fluorescence and phosphorescence measurements.

For the analytical chemist, it is of considerable practical importance that many luminescent compounds exhibit enhanced or changed emission characteristics in solutions of detergent micelles. Intensity enhancements in excess of two orders of magnitude may be encountered in fluorescence analyses when micellar media are used. In addition, the micro-organized environment can provide conditions that make room-temperature phosphorescence possible. In the case of chemiluminescence, the micellar phase can be used to circumvent mismatches in solution conditions required by sequential reactions involved in these processes. Micellar systems may be used in fluorescence sensitization and quenching measurements to provide analytical possibilities that are otherwise unavailable.

KEY WORDS: luminescence spectroscopy, micellar solution, surfactant, aggregation number, critical micelle concentration, microviscosity, reverse micelle, time-resolved fluorometry, fluorescence enhancement, fluorescence quenching, fluorescence anisotropy, chemiluminescence, room temperature phosphorescence.

I. INTRODUCTION

The interface between fluorescence spectroscopy and micro-organized environments may take two forms. First, the organized systems may have a definite (hopefully, analytically beneficial) influence on the observed fluorescence characteristics of compounds of interest. Examples include fluorescence enhancement and fluorescence quenching of analytes or interfering substances in micellar solutions. The practicing spectroscopist may therefore find the use of micellar solutions advantageous with regard to improving such matters as analytical sensitivity and selectivity. Second, fluorescence spectroscopy may be used as a tool for elucidating the nature of the organized phase. Examples of this relationship include the determination of critical micelle concentrations, micellar sizes, shapes, structures, microviscosities, and aggregation numbers by luminescence measurements. Fluorescence intensities, intensity ratios, quenching, lifetimes, and polarization are variously used for these purposes. In this context, the surface chemist uses fluorescence to gain insight into the organization of solutions containing amphiphilic species.

A number of texts and reviews dealing with micelles in analytical chemistry and with micellar photochemistry/physics have appeared in recent years.[1–8] The subject is a very broad one and exhaustive coverage within the page limits of a review article is difficult to attain. The various articles therefore have widely different areas of emphasis, often dictated by the organization of topics chosen by the authors. The present review is organized in a manner that aims to address two formal questions: (1) how can luminescence be used to understand micelles, and (2) how can micelles aid luminescence analysis?

To establish a basis of discussion, it is first necessary to define the relevant techniques and

1040-8347/92/$.50

phenomena in luminescence spectroscopy and surfactant chemistry. What follows under the heading *Background* is therefore a brief synopsis of important matters relating to both fields of study.

II. BACKGROUND

A. Luminescence

1. Fluorescence and Phosphorescence

The principles of luminescence spectroscopy are discussed in great detail in a number of excellent texts.[9–13] In this review, only a brief overview of the three major categories of luminescence spectroscopy — fluorescence, phosphorescence, and chemiluminescence — is presented.

All luminescence is the result of a radiative transition of an electronically excited molecule, atom, or ion to a state of lower energy. This requires the prior excitation, usually through the absorption of a photon of light, but variously in the form of electrical, mechanical, thermal, acoustic, or chemical energy. The transitions involved are schematically represented in the energy-level (Jablonski) diagram shown in Figure 1. In a typical scenario, the absorption (excitation) transition originates from the singlet ground state (S_0) and promotes the species to an excited singlet state (S_1, S_2, etc.). The process is fast, typically taking about 10^{-15} s. Excitation to a state above S_1 leads to a rapid (10^{-12} s) internal conversion (IC) to the first excited singlet state. Within S_1, the species vibrationally relaxes to the lowest vibrational level.

An excited species in S_1 may return to S_0 by collisional deactivation, which is a radiationless process. Alternatively, it may enter the triplet manifold by flipping one electron spin (intersystem crossing [ISC]), which is also nonradiative and is formally forbidden since it involves a change of multiplicity. A third possibility is a return to the ground state through the emission of a photon, and this is termed *fluorescence*. Depending on the fluorophore, fluorescence emission occurs 10^{-12} to 10^{-8} s after excitation.

A molecule that undergoes ISC descends into a triplet state (T_1), whence it can only return to S_0 by flipping another electron spin. The entire deactivation therefore requires two formally forbidden transitions, imparting a long lifetime to such an excited species. This enhances the probability of radiationless deactivation, especially in $T_1 \rightarrow S_0$. The radiative version of that transition, termed *phosphorescence*, is therefore rarely observed at room temperature. Rigid matrices, such as those obtained at cryogenic temperatures, are usually required to prevent collisional deactivation of all T_1 states. Alternatively, the phosphor may be immobilized through adsorption, chemisorption, or inclusion in organized media. Phosphorescence lifetimes are typically in the range 10^{-4} to 20 s. *Chemiluminescence* is a variant of fluorescence, in which the excited species is generated by a chemical reaction. The reactions that have this property are usually divided into two classes — enzymatic and nonenzymatic, the former comprising the large subclass of bioluminescence reactions. The fluorophores involved in these processes may be species that partake in the reaction and are excited in its course, or they may be extraneous dyes that derive the energy from an excited species formed in the reaction.

There are many luminescent compounds that can be used to probe micellar environments and it is beyond the scope of this review to provide an exhaustive list. A selection of useful fluorophores that have been used in recent studies is presented in Table 1. Pyrene is undoubtedly the most widely used fluorescence probe for organized media because of the well-established variation of its emission spectrum with the polarity of its immediate surroundings. The defined parameter is the ratio of the first (372 nm) and third (383 nm) peaks in the spectrum (I_1/I_3), which exhibits a continuous change with polarity, ranging from 1.89 in DMSO to 0.56 in methylcyclohexane.[14] The effect is due to vibronic coupling of the 0–0 band at 372 nm and consequent perturbations in intensity, equivalent to the Ham effect in benzene.[15,16] There are several other probes that exhibit polarity-dependent spectral characteristics, including 4-(9-anthryl)-*N*,*N*-dimethylaniline (ADMA), 3-hydroxyflavone, pyrene-3-carboxaldehyde, diphenylbutadiene, *tetrakis*(sulfonatophenyl) porphyrin (TPPS), and dibutylaminostilbazolium butylsulfonate (see Table 1).

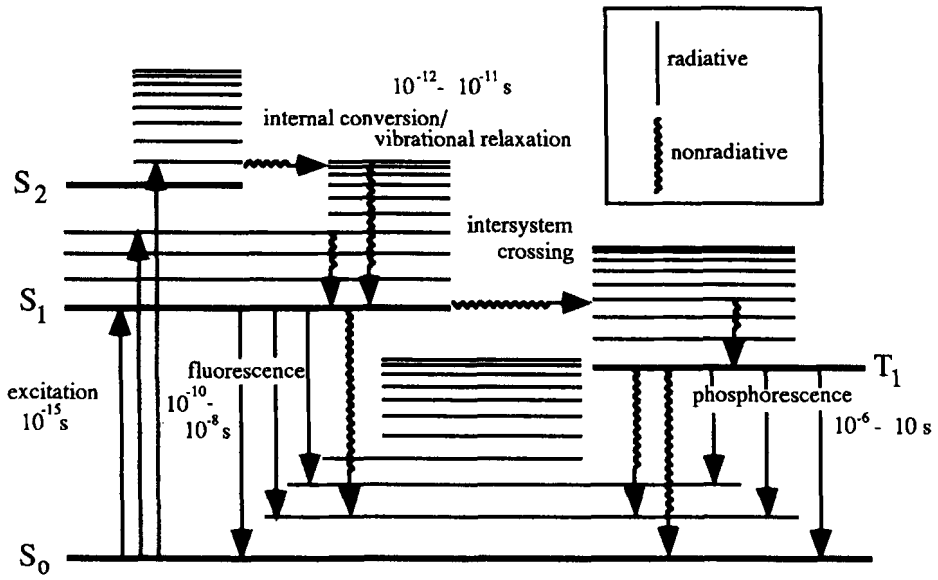

FIGURE 1. Simplified energy-level (Jablonski) diagram.

When a fluorophore is excited with plane polarized light, the emission will also be plane polarized, provided that the molecule does not undergo rotational motion during the lifetime of the excited state. To what extent this condition is met depends on the motional relationship between the fluorophore and the surrounding solution, especially the viscosity of the solvent and the size and conformation of the molecule. The essence of the interaction arising from these two parameters is the *viscous drag* that the solvent exerts on the molecule, thereby hindering its rotational diffusion. The extent of emission polarization, or "fixedness," of the fluorophore in solution may be given by two related quantities, the fluorescence polarization, *p*, and the fluorescence anisotropy, *r*; they are given by Equations 1 and 2, respectively,

$$p = \frac{I_{//} - I_{\perp}}{I_{//} - I_{\perp}} \quad (1)$$

$$r = \frac{I_{//} - I_{\perp}}{I_{//} - 2I_{\perp}} \quad (2)$$

where $I_{//}$ is the fluorescence intensity measured with excitation and emission polarizers set parallel, while $I_{\perp}$ is the intensity with the polarizers adjusted perpendicular to each other. The factor 2 in the denominator of Equation 2 arises because there are two components that are perpendicular to plane polarized excitation: one is readily measurable, but the other is not measurable because it lies in the line of propagation of the radiation. Given random motion of the fluorophore in solution, the two components will have equal magni-

TABLE 1
Fluorescent Probes

Probe	Excitation wavelength (nm)	Emission wavelength (nm)	Φ_f	Ref.
Anthracene	350	398	0.3	17, 18
6-(9-Anthroyloxy)stearic acid	337	460		19
4-(9-Anthryl)-*N,N*-dimethylaniline	366	400	0.8	20
Benzo[a]pyrene	381	403	0.42	21, 22
Biphenyl	280	313	0.15	21, 23
1,3-*bis*(1-Pyrenyl)propane	340	378		24
Chrysene	264	380	0.17	18, 25
Dibutylaminostilbazolium butylsulfonate	425	626		26
Diphenylbutadiene	328	370		18, 27
Fluoranthene	354	464	0.21	17, 22
Fluorene	300	325	0.54	17, 18
Fluorescein	494	515	0.92	17
3-Hydroxyflavone	340	411, 514		28
Methyl-9-anthroate	337	455	0.75	29
1-Methylpyrene	330	390		30
n-butyl-b-naphthalimide	362	415		31
Naphthalene	276	320	0.12	17, 32
1-Naphthol	312	449		33
Perylene	410	472	0.98	25, 34
Phenanthrene	252	360	0.1	17, 18
Pyrene	335	380	0.65	17, 25
Pyrene-3-carboxaldehyde	380	469		35
Rhodamine B	535	605	0.97	17
Tetracene	366	474		36
Tetrakis(sulfanatophenyl) porphyrin	337	650	0.17	37
Tris(2,2'-bipyridyl)ruthenium(II)	285	598		38

tude. Cursory inspection of Equation 2 suggests that the anisotropy of a perfectly scrambled solution (i.e., where complete depolarization occurs during the excited lifetime) equals zero, while a perfectly vitreous solution has r = 1. The latter is not the case because photoselection during the excitation process leads to a fundamental anisotropy, r_0, given by

$$r_0 = \frac{3\cos^2\theta - 1}{5} \qquad (3)$$

where θ is the angle between the excitation and emission oscillators of the fluorophore. In the relatively rare cases where the two oscillators are collinear (θ = 0), *r* can reach a maximum value of 0.4; in all other cases, it is smaller. Measurement of the fluorescence anisotropy of a species in solution allows for an assessment of its Brownian motion, which may lead to subsequent deductions concerning its size, conformation, or adsorptive attachment. The relation between the anisotropy and the rotational relaxation time, ρ, of a solute is given by the Perrin equation

$$\frac{r_0}{r} = 1 + \frac{\tau}{\rho} \qquad (4)$$

where τ is the fluorescence lifetime.

2. Sensitization

Sensitized fluorescence emission is obtained when the fluorophore (acceptor) is excited by transfer of energy from a primary absorber (donor). The two main requirements for this to happen are that there be an energy match between the

two species involved and that they be sufficiently close to each other to make it possible. A frequently used relationship to describe the energy transfer efficiency, E, is[39]

$$E = \left[\frac{G(\lambda_1)}{G(\lambda_2)} - \frac{\varepsilon_A(\lambda_2)}{\varepsilon_A(\lambda_1)}\right]\frac{\varepsilon_A(\lambda_1)}{\varepsilon_D(\lambda_2)} \qquad (5)$$

where $G(\lambda)$ is the magnitude of the corrected excitation spectrum of the energy acceptor excited at wavelength λ. Molar absorptivities are symbolized by ε, and the subscripts A and D refer to the energy acceptor and donor, respectively. G is measured at two wavelengths: λ_1 where the donor has no absorption, and λ_2 where the absorptivity of the donor is large compared to that of the acceptor.

The distance between donor and acceptor, R, is given by

$$R = R_0\left(\frac{1}{E} - 1\right)^{1/6} \qquad (6)$$

where R_0 is the Förster distance, that is, the distance at which the energy transfer efficiency is 50%. The expression for R_0 is

$$R_0^6 = 8.785 \times 10^{-25} k^2 Q_D n^{-4} J(\nu) \qquad (7)$$

where n is the refractive index of the intervening medium, k^2 is the orientation factor, Q_D is the quantum efficiency of the fluorescence donor, $J(\nu)$ is the overlap integral, and N is Avogadro's number. The value of k^2 is usually taken as 2/3 if the donor and acceptor are free to rotate during the excited-state lifetime of the donor.[40] The value of Q_D can be calculated[41] from Equation 8

$$Q_D = \frac{\text{(area under emission spectrum of donor)}}{\text{(area under emission spectrum of quinine sulfate)}} \times \frac{0.70(A_{252} \text{ for quinine sulfate})}{A_{252} \text{ for donor}} \qquad (8)$$

where A_{252} is the absorbance at 252 nm. The overlap integral is

$$J = \int \frac{F_D(\nu)\varepsilon_A(\nu)d\nu}{\nu^4} \qquad (9)$$

where F_D is the fluorescence intensity of the donor and ν is the frequency. The value of the integral may often be determined by Simpson's rule.

3. Fluorescence Quenching

Fluorescence is said to be quenched when an interaction between the fluorophore and another species leads to a diminution, or even elimination, of the fluorescence signal. This interaction may take place in the excited state of the fluorescent compound and be collisional in nature, in which case it is referred to as *dynamic quenching*. The excitation energy is transferred to the quencher and usually nonradiatively dissipated. Alternatively, the fluorophore and the quencher may associate in the ground state, forming a species that lacks the original fluorescence characteristics. This is termed *static quenching*.

Quenching interactions are described by the Stern-Volmer equation:

$$F_0/F = 1 + K_D[Q] \qquad (10)$$

where F_0 is the fluorescence intensity in the absence of quencher and F the quenched intensity, K_D the Stern-Volmer quenching constant, and [Q] the quencher concentration. The equation holds for both dynamic and static quenching, with the proviso that only one type of quenching is operative and that the fluorophore is present as a single population. Linear Stern-Volmer plots (F_0/F vs. [Q]) are obtained under those circumstances.

In the case of dynamic quenching, the slope of the plot K_D is $\tau_0 k_q$, where τ_0 is the unquenched fluorescence lifetime and k_q is the bimolecular quenching constant. For such a collisional process, the quantity F_0/F may be replaced by τ_0/τ, where τ is the fluorescence lifetime in the presence of quencher. For static quenching, K_D becomes the binding constant of the ground-state complex between fluorophore and quencher.

In micellar environments, fluorescence quenching may be useful to eliminate unwanted luminescence, as for resonance Raman measurements,[42,43] or it may be actively utilized to determine micellar aggregation numbers.

B. Micelles[44-46]

Micelles are colloid-sized conglomerates of surface-active species in solution. For normal micelles, the dispersion medium is usually water and the individual surfactant molecules or ions aggregate to minimize interfacial energies. In the resulting bodies, the hydrophilic "heads" of the surfactant face the aqueous solution, while the hydrophobic "tails" project inward, facing each other. The result is an assembly that resembles a miniature oil drop, comprising a lipophilic microphase (pseudophase) in the aqueous bulk.

Micelle formation starts at a narrow and characteristic range of detergent concentration, termed the *critical micelle concentration* (cmc). The value of the cmc, the number of monomers that aggregate, and the eventual size of the micelle are all critically dependent on the nature of the aggregating species. Typical cmc values are in the range 10^{-4} to 10^{-2} *M*, aggregation numbers at the cmc vary from ca. 40 to 150, and micellar dimensions (diameters of nominally spherical species) are 20 to 120 Å. Aggregation numbers and sizes are also highly dependent on surfactant concentration, the presence of other species in solution, and the temperature. Micelles grow with increasing surfactant concentration, often changing shape as they increase in size. The majority of ionic detergents, for instance, form spherical micelles near the cmc, but become rod-like in shape at higher concentrations. Addition of electrolytes, as well as neutral species such as alcohols and hydrocarbons, likewise tend to increase micellar sizes and aggregation numbers. A list of selected surfactants and their characteristic parameters is presented in Table 2. Phospholipids and related surfactants tend to form more elaborate bilayer aggregates that arrange themselves into single or double compartment vesicles, aligned around a central aqueous pool. Structures of this type are the building units of biological lipid membranes.

1. Microemulsions

Microemulsions are variously viewed as swollen micelles[47] or as distinctly different systems.[48] They consist of microdroplets of the dispersed phase, stabilized by surfactants exposed on their surface. They may be of the oil-in-water (o/w) or water-in-oil (w/o) type, and the droplet diameters are typically less than 1000 Å, rendering the solutions optically transparent. Microemulsions are an important medium in their own right, but they will not be considered further in this review. The various types of microorganized systems are summarized in Figure 2.

2. Temperature

The effect of temperature on dissolution and micellization differs for different classes of surfactants. Ionic detergents have an upper consolute temperature, called the *Krafft point*, T_k, at which their solubilities undergo a sharp increase. Monomer solubility proceeds to increase above T_k, continuing up to and beyond the cmc. Values of T_k range from as low as 8°C for $C_{10}H_{21}COOC(CH_2)_2SO_3Na$ to as high as 80°C for *n*-$C_8F_{17}SO_3K$. Nonionic detergents, most of which are liquid or semi-liquid, have a lower consolute temperature, referred to as the *cloud point*. At the cloud point, micelles coalesce to form macroscopic aggregates and solutions separate into detergent-rich and detergent-poor phases. In the latter, the surfactant remains at the cmc, while it is the main component in the former. Dehydration of the hydrophilic portion of the detergent molecule is thought to be the cause of this phenomenon. Cloud points vary widely with detergent, ranging from 20 to 90°C.

3. Reverse Micelles

Micelles of surfactant species can also form in nonaqueous solvents of low polarity. The monomers in these *reverse*, or *inverse*, *micelles* are oriented in the opposite sense to those in normal micelles (Figure 1), with the hydrophilic moieties projecting inward and the hydrophobic ones outward. Reverse micelles generally form around

TABLE 2
Surface Active Agents

Surfactant	Common name/ abbreviation	CMC (m*M*)	Aggregation number
Anionic			
Sodium *bis*(2-ethylhexyl)sulfosuccinate	Aerosol OT (AOT)		
Sodium dodecyl (or lauryl) ether sulfate	SDES (SLES)		
Sodium dodecyl (or lauryl) sulfate	SDS (SLS, NaLS)	8	62
Sodium dodecyl benzene sulfonate	SDBS		
Sodium oleate			
Sodium stearate			
Sodium taurocholate	NaTC	10–15	4
Cationic			
Benzalkonium chloride	BAC	6	
Benzyldimethylalkylammonium bromides			
Cetyl trimethylammonium bromide	CTAB	0.92	60
Cetyl trimethylammonium chloride	CTAC	1.4	105
Dodecyl trimethylammonium bromide	DTAB	14	
Dodecylamine hydrochloride	DAH		
Dodecyldimethylammonium chloride	DODAC		
Hexadecyl trimethylammonium bromide	HDTB	0.026	169
Hexadecyl trimethylammonium chloride	HTAC		
N-Cetylpyridinium bromide	CPyC	0.9	
Nonionic			
Alkanoyl-N-methylglucamides	MEGA-7, -9, -10		
n-b-D-glucopyranosides		25 (octyl)	27
Polyoxyethylene sorbitans (Tweens)			
Polyoxyethylene ethers such as:			
Brij series: Brij 35, 56, 99, etc.		0.06 (Brij 35)	40
Triton series: Triton X-100, X-114, etc.	TX-100, etc.	0.24 (TX-100)	140
Polyoxyethylene(E9-10)nonyl phenol	IGEPAL CO-630	0.046	150
Sorbitans (e.g., Spans)			
Nonylphenol-ethylene oxide condensates	Nemol K-series		
Ethylene oxide-propylene oxide condensates	Genapol PF-series		
Poly(ethylene glycols)	PEG series		
Zwitterionic			
(3-[(3-Cholamidopropyl)-dimethylammonium]-1-Propanesulfonate	CHAPS	8	10
Dodecyl betaine			
N-dodecyl-*N,N*-dimethyl-3-ammonium-1-Propanesulfonate	Sulfobetain 12 (SB12)		

Data taken from References 44 to 46 and references therein.

internal water pools that solubilize the polar head groups of the detergent. The amount of water present, expressed as the water/detergent ratio, w, determines the size of the water pool and hence the micellar diameter. As w is increased, the classification of the aggregate moves from reverse micelle to water-in-oil microemulsion, the distinction being mostly one of size. Aggregation numbers of reverse micelles are typically smaller than those of normal micelles, usually lying in the range of 20 to 80 monomers.

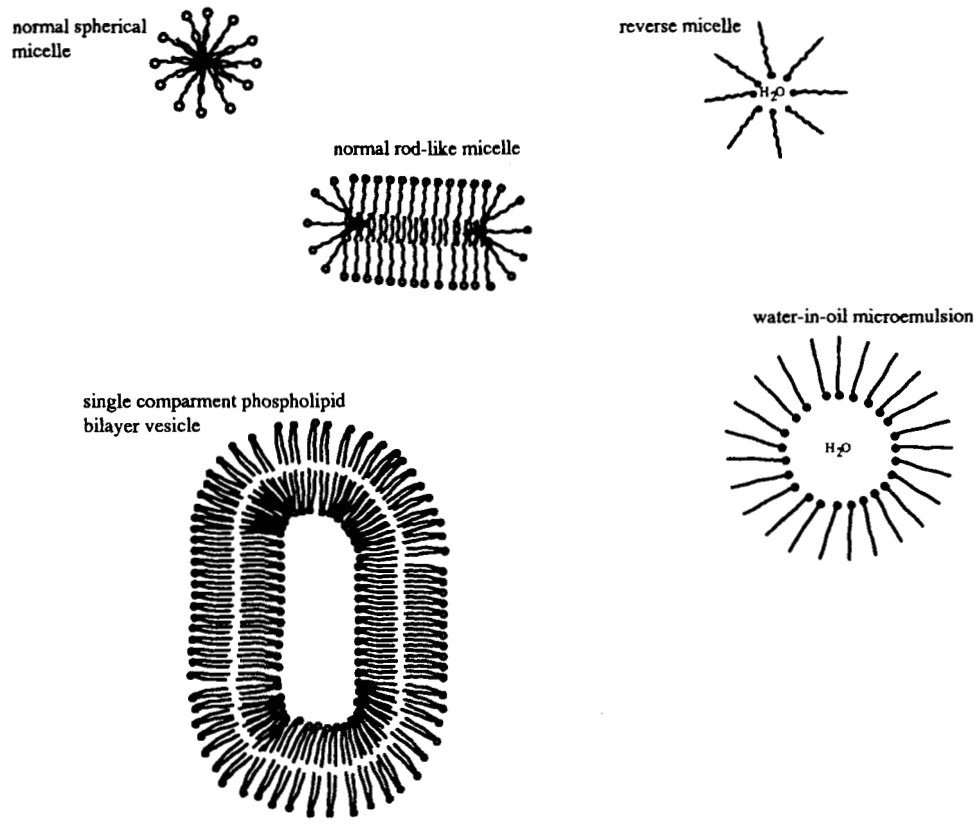

FIGURE 2. Common types of micellar aggregates.

4. Microviscosity

The micellar interior, being a distinctly different phase than the bulk solvent, differs from it in viscosity. The term *microviscosity* is normally used for the micellar phases in accordance with its relative dimensions. The structured nature of the micelle interior usually causes it to be more viscous than a comparable (e.g., hydrocarbon) macrophase because of motional restraints in the palisade layer of the micellized surfactant. For instance, the viscosity of dodecane at 25°C is 1.35 cp, while the value for the interior of a sodium dodecyl sulfate micelle at that temperature is about 12 cp.[49] Similarly, hexadecane at 20°C has η = 3.34 cp, but the interior of a hexadecyl-trimethylammonium chloride (CTAC) micelle it is 31 cp.[50] It should also be noted that the detergent counterion in ionic micelles can have a surprising influence on the viscosity of the interior. CTAB, the bromide analogue of CTAC, gives a micellar microviscosity of 39 cp under similar conditions.

5. Micellar Distribution

A study of luminescence in micellar solutions inevitably deals with fluorophores that distribute themselves between the micellar microphase and the bulk solution. The macroscopic manifestation of phenomena that are peculiar to species located in the interior of micelles is dependent upon the extent of this occupancy. It has been found[51,52] that the distribution of probe molecules over micelles is described by Poisson statistics, leading to the probability expression:

$$P(n) = \frac{\langle N \rangle^n e^{-\langle N \rangle}}{n!} \qquad (11)$$

where P(n) is the probability of finding a micelle containing n probe molecules and $\langle N \rangle$ = [probe]/

[micelle]. P(n) describes a random distribution, allowing for multiple occupancy that is independent of the number of species present in the micelle. This necessarily limits the value of ⟨N⟩ inasmuch as too many extraneous species clearly disturb the micellar structure and its ability to accept more "riders."

III. LUMINESCENCE IN MICELLES

A. Critical Micelle Concentrations

The determination of the cmc by fluorescence measurements is well established and is only mentioned briefly here. The technique requires a change in emission/excitation characteristics upon micellization of a probe[53,54] and these may involve quantum yields, lifetimes, protection from quenching, spectral shifts, or vibronic band variations arising from the Ham effect. Fluorescent dyes are useful for cmc determinations because large spectral changes often accompany their incorporation in micelles.[55] However, caution must be exercised because the charge and concentration of the dye can affect the apparent cmc obtained. In a recent study on poly(styrene-ethylene oxide) block copolymer micellization,[56] a red shift of the pyrene excitation spectrum, a decrease of its I_1/I_3 vibronic band ratio from 1.9 to 1.2, and a lifetime increase from 200 to 350 ns were used to determine the cmc at 1 to 5 mg/l.

B. Micellar Aggregation Numbers

The use of fluorescence quenching for the determination of micellar aggregation numbers was introduced by Turro and Yekta.[57] Their method is based upon a static quenching process in which both the quencher Q and the fluorophore D reside exclusively in the micellar phase. Both species are distributed among the micelles according to Poisson statistics; if both are present in a micelle, fluorescence is completely quenched. Emission is therefore observed only from micelles that contain D but do not contain Q. The micelles from which emission is observed are assumed to be monodisperse in size. The quenched (I) and unquenched (I_0) fluorescence intensities are related to quencher concentration [Q] and micelle concentration [M] by the simple expression

$$\frac{I}{I_0} = e^{-[Q]/[M]} \tag{12}$$

The micelle concentration can be related to the mean aggregation number, N, by

$$[M] = \frac{[Det] - [free\ monomer]}{N} \tag{13}$$

where [Det] is the analytical detergent concentration and [free monomer] is the concentration of detergent not contained in aggregates (i.e., the cmc). A combination of Equations 12 and 13 gives

$$[\ln(I_0/I)]^{-1} = \frac{[Det] - [free\ monomer]}{[Q]N} \tag{14}$$

and a plot of $[\ln(I_0/I)]^{-1}$ vs. [Det] has a slope of $([Q]N)^{-1}$ and hence yields N. The method has been shown to be fairly accurate for small micelles with aggregation numbers up to about 120.[58,59]

A similar treatment,[60] which presumes that the quencher is wholly solubilized in the micelle, leads to the expression

$$\frac{I}{I_0}(1 + R_0) - R_0 = e^{-\bar{n}} \tag{15}$$

where $R_0 = I_{wo}/I_{mo}$, the ratio of intensities of the aqueous probe and the micellized* probe in the absence of quencher, and $\bar{n} = [Q]/[M]$. A plot of $-\ln(I(1 + R_0)/I_0 - R_0)$ vs. [Q] will therefore be linear and provide [M] and hence the aggregation number.

Micellar aggregation numbers may also be determined by time-resolved fluorescence quenching (TRFQ) measurements,[61] which is relevant to dynamic quenching situations. This technique is applicable to larger micelles (N > 120), and it

* The term "micellized," applied to a fluorescent probe, refers to its presence in the micelle interior.

should yield values of N that are independent of micellar shape, intermicellar interactions, and quencher concentration. However, it is also subject to the assumption that micellar solutions are monodisperse.[62] As this is never the case, a mean aggregation number $\langle N \rangle$ is in fact determined. If polydispersity is low, this may be taken as a number-average aggregation number.[63] More recent theory[64] has shown that for polydisperse micelles, the quenching-average aggregation number, designated $\langle N \rangle_Q$, depends on [Q] ($\langle N \rangle_Q$ decreases with increasing [Q]). An explanation for this, invoking double micellar distribution, has been provided.[65]

In TRFQ, N is determined from the fluorescence decay curve of a micellized probe. In monodisperse micelles, the intensity decays according to the equation (sometimes referred to as the Infelta equation):

$$I(t) = I(0)\exp\{-A_2 t - A_3[1-\exp(-A_4 t)]\} \quad (16)$$

where I(t) and I(0) are the fluorescence intensities at times t and 0, while A_2, A_3, and A_4 are time-independent parameters. These parameters are determined empirically by fitting Equation 15 to the data.

In situations where intermicellar movement of probe and quencher molecules is slow relative to the excited lifetime, the A-parameters become: $A_2 = k_0$, $A_3 = [Q]/[M]$, and $A_4 = k_q$. Here $k_0 = 1/\tau_0$, the fluorescence decay rate constant of the micellized probe in the absence of quencher; k_q is the pseudo-first-order rate constant of intramicellar quenching of probe fluorescence.

For the determination of the aggregation number, A_3 is the parameter of interest since, as with static quenching, N can be expressed in terms of the relevant concentrations. This becomes

$$N = \frac{(C - cmc)A_3}{[Q]} \quad (17)$$

An empirical determination of A_3 therefore yields the aggregation number.

The TRFQ method was recently used by Reekmans et al.,[66] to investigate the influence of alkanes and alcohols on the aggregation of ionic surfactants. They found that alkanes and long alcohols increase the aggregation number of SDS (sodium dodecyl sulfate) and DTAC significantly, while smaller alcohols (≤C7) have a less pronounced effect and butanol actually decreases the aggregation number.

A somewhat modified version of TRFQ, involving fluorescence donor and acceptor dyes in a micellar environment, has recently been used to measure micelle sizes and aggregation numbers. This is discussed below in Section D.

A third method for the fluorimetric determination of micellar aggregation numbers was first reported by Atik et al.[67] They derived an expression for the time-dependent monomer fluorescence of a probe such as pyrene, which can form excimers in micelles

$$\ln(I_M / I_M^0) \approx -(\bar{n} + k_1 t) \quad (18)$$

where I_M and I^0_M are the monomer fluorescence intensities at time t and 0, respectively, $\bar{n}$ is the average number of fluorophores per micelle, k_1 is the intramicellar first-order decay constant of the excited species, and time t is long for this approximate expression to hold. Extrapolation of a plot of $\ln(I_M/I^o_M)$ vs. t to t = 0 therefore gives $-\bar{n}$. In turn, $\bar{n} = [F_T]/[M_T]$, where $[F_T]$ and $[M_T]$ are the total fluorophore and micelle concentrations. Since $[F_T]$ is under control of the experimenter, the value of $[M_T]$ is obtained, and, combined with the total detergent concentration C, yields the average aggregation number. This method has been used[68] to assess the influence of NaCl on the size of SDS micelles ($Ru[bpy]_3^{2+}$ was the probe), and it was found that the aggregation number increases dramatically at salt concentrations above 0.45 *M*.

C. Microviscosities

The microviscosity of the micellar interior is a parameter of considerable interest since it has a profound effect on the diffusive motion of micellized species, and hence on their reactivities and spectral properties. The term refers to effects that limit short-range molecular rearrangement of species on time scales that are typically shorter than 1 ms. The determination of microviscosities,

with special reference to phospholipid membranes, has been extensively described in an early paper by Cogan et al.[69] They used perylene, 2-methylanthracene, and 9-vinylanthracene as their fluorescent probes; diphenylhexatriene (DPH) is another useful fluorophore for this purpose.[9,70]

Microviscosities may be determined by a steady-state approach in which the fluorescence anisotropy, r, (*vide supra*) of the micellized probe is measured. This value, typically expressed as a ratio with the limiting anisotropy (r_0/r), is compared to a calibration curve obtained with reference solvents of known viscosity. Figure 3 shows such a calibration curve.

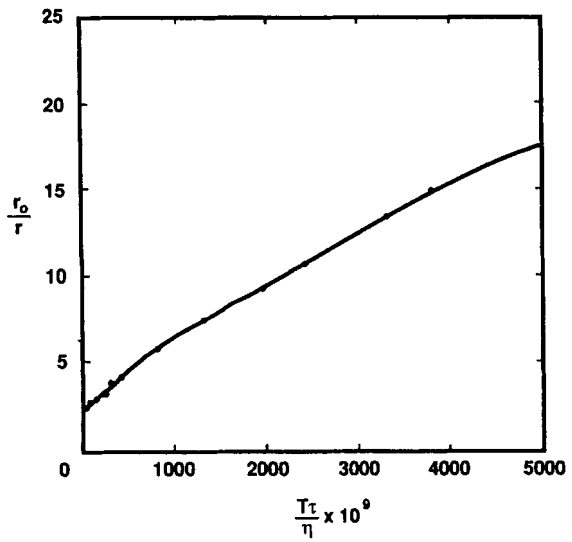

FIGURE 3. Dependence of r_0/r on $T\tau/\eta$ for perylene. T, absolute temperature; η, viscosity; τ, decay time of excited state; r obtained in White Oil USP 35; r_0 obtained inpropylene glycol at –50°C (From Cogan, U.; Shinitzky, M.; Weber, G.; Nishida, T. *Biochemistry.* **1973,** *12,* 521. With permission.)

It is implicit in this technique that the surroundings of the micellized probe are considered to be essentially identical to the reference bulk liquid. While that is a fair approximation in many cases, it is not always strictly true. Discrepancies have been shown to exist by measurement of time-resolved fluorescence anisotropies. Work by Dale et al.[71,72] has shown that, while r(t) of a probe (diphenylhexatriene) in mineral oil decays to zero, in a micro-organized phospholipid vesicle it reaches a higher limiting value (Figure 4). This indicates that the probe experiences hindered diffusive motions in the structured environment.

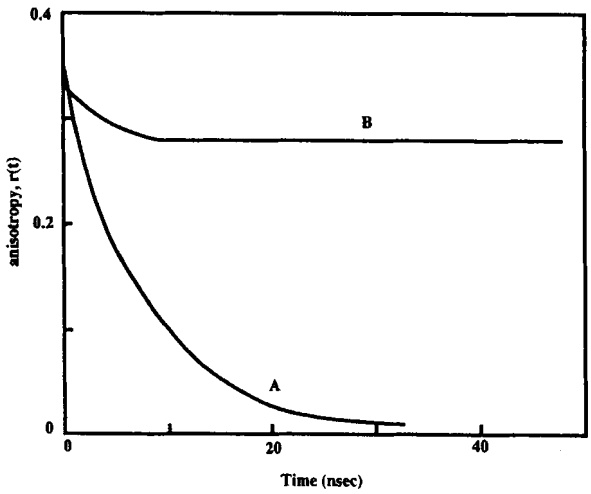

FIGURE 4. Time-resolved fluorescence decays of diphenylhexatriene: (A) in mineral oil at 16°C; (B) in phospholipid vesicles of dimyristoyl-L-α-phosphatidylcholine at 14.8°C. (Adapted from Dale, R.E.; Chen, L.A.; Brand, L. *J. Biol. Chem.* **1977,** *252,* 7500. Chen, L.A.; Dale, R.E.; Roth, S.; Brand, L. *J. Biol. Chem.* **1977,** *252,* 2163. With permission.)

A second, possibly simpler, way of determining micellar microviscosities is by measurement of excimer/monomer emission ratios (E/M) of intramolecular excimer-forming probes. Zachariasse,[73] using 1,3-*bis*(1-pyrenyl)propane (DPyP), was the first to demonstrate that E/M is a measure of the microviscosity in situations where excimer formation takes place. The technique has been used fairly extensively since then, both with DPyP[74–76] and with other probes.[49,50,77] It requires only the measurement of monomer and excimer emission intensities of the probe in the test environment, followed by a direct determination of its microviscosity by reference to standards of known viscosity. Recently, Parthasarathy and Labes[24] have extended the use of DPyP E/M ratios to lyotropic mesophases (liquid crystals). They note in their report that the variation of E/M with detergent (sodium decyl sulfate [SDecS]) concentration in micellar solutions is exponential

(Figure 5). The explanation for this is that increased detergent concentration leads to increased aggregation number and decreased surface area per head group. The improved packing of the alkyl moieties leads to increased microviscosity and reduced excimer yield.

tions[80] and provides no internal check on the applicability of the Debye-Stokes-Einstein (DSE) model to the fluid. The relative values of D_x, D_y, and D_z, on the other hand, reveal both the boundary conditions and the viscous continuum nature of the system.

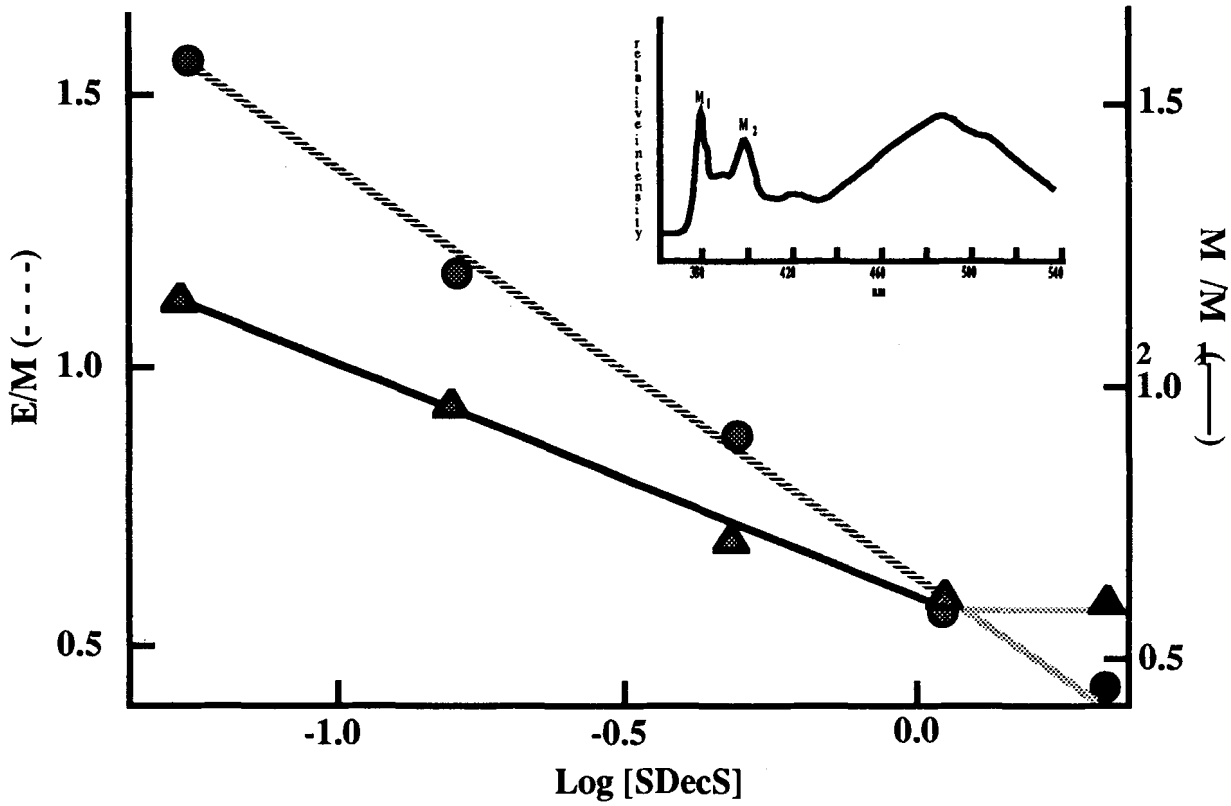

FIGURE 5. Plots of E/M and M2/M1 of DPyP vs. log[SDecS]. Inset: emission spectrum of DPyP. (From Parthasarathy, R.; Labes, M.M. *Langmuir.* **1990,** *6,* 542. With permission.)

The rotational diffusion of species associated with micelles is a central feature of the concept of micellar microviscosity. Detailed studies of the rotational behavior of fluorescent probes in micelles have been carried out by Wirth and coworkers.[78,79] They note that rotational diffusion provides more information about microviscosity than translational diffusion, inasmuch as the former provides three degrees of freedom: D_x, D_y, and D_z, the rotational diffusion coefficients for the three solute axes. Translational diffusion gives only one degree of freedom, D_t, which contains no clue regarding slip or stick boundary condi-

The rotational diffusion coefficient, D (the average of D_x, D_y, and D_z) is related to the viscosity, η, by the expression

$$\frac{D}{6} = \frac{\eta V}{kT} f_{stick} C \qquad (19)$$

where V is the hydrodynamic volume of the solute, kT is the thermal energy, f_{stick} is a geometric factor,[81] and C is a solute-solvent interaction parameter.[82,83] D is determined fluorometrically by use of a relation derived by Chuang and Eisenthal.[84] In its complete form, this is a five-

component exponential, but it can reduce to a double exponential decay for flat, symmetrical molecules:

$$r(t) = 0.3(\cos^2\theta - 1/3 - (D_x + D_z\cos^2\theta + D_y\sin^2\theta - 2D)/\Delta)\exp(-(6D - 2\Delta)t) + 0.3(\cos^2\theta - 1/3 + (D_x + D_z\cos^2\theta + D_y\sin^2\theta - 2D)/\Delta)\exp(-(6D - 2\Delta)t) \quad (20)$$

where

$$\Delta = (D_x^2 + D_y^2 + D_z^2 - D_xD_y - D_xD_z - D_yD_z)^{1/2} \quad (21)$$

r(t) is the time-resolved fluorescence anisotropy and θ is the angle between the excitation and emission transition moments.

D. Micellar Sizes, Shapes, and Structures

To determine the sizes of micelles by fluorometry or any other method, the theory describing the technique obviously needs to comprise an explicit size parameter, such as the micellar diameter in the case of spherical micelles. In fluorescence, this parameter presents itself most clearly in the case of micellar resonance energy transfer, in which an excited donor sensitizes the fluorescence of an acceptor, both contained in a micelle. The distance between the two species is a deciding factor in the efficiency of the energy transfer, and it is in turn related to the dimensions of the micellar microreactor in which the process takes place. This is only true because of the restricted nature and relatively small size of this environment, which allows the approximation that donor and acceptor are separated by a fixed distance.

Choi et al.[85] have given an excellent account of the application of picosecond resonant energy transfer measurements to the determination of the diameter of spherical SDS micelles. In the theory developed by Förster,[86] the energy transfer rate constant, k, is given by:

$$k = \frac{1}{\tau_0}\left(\frac{R_0}{R_{da}}\right)^6 \quad (22)$$

where τ_0 is the donor fluorescence lifetime in absence of an acceptor (quencher), R_{da} is the donor-acceptor separation, and R_0 is the Förster radius (i.e., the characteristic distance at which the transfer efficiency is 50%). R_0 is given in Equation 7.

Choi and co-workers[85] used rhodamine 6G as the donor and malachite green as the acceptor. Both are cationic dyes and, in a solution of anionic SDS micelles, they are adsorbed to the micellar surface. Under those circumstances, the probability of finding an acceptor at a distance R from a donor is proportional to R.[87] Assuming a Poisson distribution of dye molecules over the micelles, the time-dependent probability of finding an excited acceptor is given by:

$$p_a(t) = e^{-t/\tau_0}\sum_n \frac{\langle n\rangle^n e^{-\langle n\rangle}}{n!}\left\{\int_0^{2R_m}\exp\left[\frac{-t}{\tau_0}\left(\frac{R_0}{R}\right)^6 R\,dR\right]\right\}^n \quad (23)$$

where R_m is the radius of the micelle, n is the number of dye molecules per micelle, and ⟨n⟩ is the number of acceptors per micelle. The radius R_m refers to the sites within the micelle that are accessible to the probe, and the size of headgroups that lie beyond that sphere will have to be added to obtain the size of the entire body. Using Equation 23, a fluorescence time profile can be constructed for different values of R_m (Figure 6).

Comparison of calculated curves with experimentally obtained ones provides a good measure of R_m and ⟨n⟩, as long as the radius is not very much larger than R_0. A value of 22 Å was determined for the radius of SDS micelles.[85] The picosecond time-resolved technique described here also provides an alternative way of determining the micellar aggregation number, since $N = \langle n\rangle(C - cmc)/c_a$ (where C is the total detergent concentration and c_a is the acceptor concentration).

These micellar size calculations are pertinent to small spherical micelles containing one probe

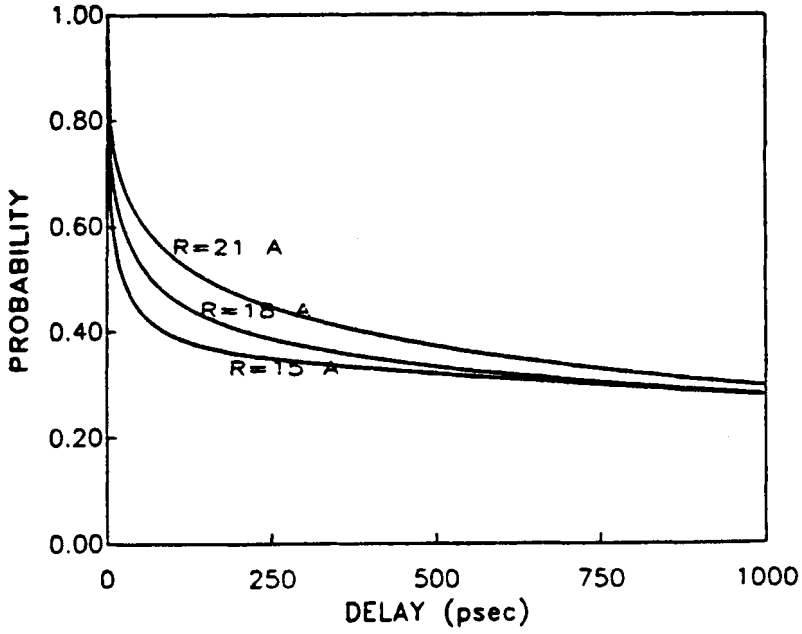

FIGURE 6. Simulated fluorescence time profiles for the rhodamine 6G/malachite green pair at fixed quencher concentration, ⟨n⟩ = 2.0, for various micelle radii R_m: 15, 18, 21 Å. (From Choi, K.-J.; Turkevich, L.A.; Loza, R. *J. Phys. Chem.* **1988,** *92,* 2248. With permission.)

and one quencher molecule. It is, however, well established that the addition of electrolytes such as NaCl can lead to aggregates that are more than 10 times larger than those not so treated.[68,85,88] Rationalization of such bodies requires that shapes other than simple spheres be invoked. The vesicle model and the cylindrical model are such shapes, and they too can be studied by time-resolved fluorescence.

Vesicle-shaped aggregates comprise a double-walled structure (Figure 2) consisting of detergent species oriented in the energetically favorable manner, surrounding a central pool of solvent. The fluorescence decay profiles for both cylindrical and vesicle micelles are given by the general equation (*cf.* Infelta Equation 16 above):

$$I(t) = I_0 \exp\left[\frac{-t}{\tau_0} - an_q\left(\frac{t}{\tau_0}\right)^{1/b}\left(\frac{R_0}{R_G}\right)^m\right] \quad (24)$$

where, for cylindrical micelles, a = 1.354, b = 3, and m = 2; for vesicle micelles, a = 1.772, b = 2, and m = 3. In the cylindrical model, R_G is the radius of a random walk traced out by the elongated, nonrigid aggregate.

Almgren and co-workers,[89,90] have conducted detailed studies on the diffusion of fluorophores and quenchers in long cylindrical (rod-like) micelles, using deactivation of both singlet and triplet states. They have derived expressions for luminescence decay in such aggregates, accounting for their polydispersity as well as the possibility of migration of quencher between them.

Fluorescence lifetimes are a powerful tool for the study of micellar organization. However, lifetime decay patterns can be extremely complex due to the heterogeneity of the fluorescence probes. This is especially true in micellar systems where polydispersity and other factors may lead to varied environments with a single type of probe. The maximum entropy method (MEM), which has found use in scientific disciplines ranging from astrophysics to tomography,[91] was introduced to pulse fluorometry by Livesey and Brochon.[92] Siemiarczuk and Ware[93] were the first to use the technique in the distribution analysis of com-

plex lifetime patterns of fluorophores in micelles, and this has provided new insights into micellar penetration by water. The method is inherently free of bias, spans a broad range of lifetimes, and allows for the accurate determination of kinetic parameters. The detailed mechanics of MEM have been carefully explained in Reference 92 and will not be reproduced in their entirety here. The process can be summarized by noting that the total fluorescence, F(t), resulting from an excitation flash is given by

$$F(t) = E(t) * \int \alpha(\tau) e^{-t/\tau} d\tau \qquad (25)$$

where E(t) is the temporal shape of the exciting flash and $\alpha(\tau)$ the decay constant at lifetime τ. The symbol * represents a convolution defined by

$$E * f = \int_0^t E(t - t') \cdot f(t') dt' \qquad (26)$$

where t and t′ refer to two different time scales related by $t = qt'$. The decay constant $\alpha(\tau)$ is the inverse Laplace transform of the measured light deconvolved by the flash E(t). This inverse transform is ill-conditioned and small errors in the fluorescence curve lead to large errors in $\alpha(\tau)$. However, a set of physically feasible solutions $\alpha(\tau)$ can be obtained, and the best member of this set should be chosen by maximizing some function $f[\alpha(\tau)]$. In MEM, this is the entropy-like function

$$S = -\sum_{i=1}^{N} \alpha_i \ln\left(\frac{\alpha_i}{\alpha_{tot}}\right) \qquad (27)$$

where N is the number of exponents and, $\alpha_{tot} = \sum_{i=1}^{N} \alpha_i$, and the condition $\chi^2 \approx 1$ exists.

Using the MEM recovery technique with pyrene in SDS micelles, Siemiarczuk and Ware[94] found significant lifetime broadening and a complex variation of lifetime distribution with detergent concentration (Figure 7).

The observed broadening and shifting of the lifetimes is probably due to the different environments that the probe can experience in a micelle. Pyrene molecules located near the surface, or those contacted by penetrated water, will encounter more polar conditions and have shorter lifetimes than those buried in the hydrocarbon region. The polydispersity of the micelles, especially at higher detergent concentrations, also influences the quality of the probe surroundings and hence its fluorescence lifetime. The monomers in large cylindrical micelles are more tightly packed than small spherical ones and the larger micelles contain less water. The presence of a mixture of different types of micelles would be expected to result in a broad lifetime distribution. Its shift toward larger values with increasing detergent concentration (micelle size) indicates a subtle decrease of polarity of the probe environment. The fact that the fluorescence lifetimes have finite widths and that they are not measured as a single average value shows that the exchange of pyrene between sites of different water content is relatively slow.

The water content of micelles can also be monitored with fluorophores containing the 9-anthroate chromophore (e.g., methyl 9-anthroate).[30] Both its quantum yield and its lifetime decrease strongly with water content (Table 3), while the emission spectrum shows a 20-nm bathochromic shift over a similar range of water concentrations. The quenching rate constant and the lifetime are independent of solvent properties other than H-bonding ability. This makes the 9-anthroates good probes for micelles as data can be extrapolated from homogeneous media, such as water-dioxane mixtures, to microheterogeneous ones.

E. Reverse Micelles

Fluorescence spectroscopy can be used to evaluate the polarity of the pool of solubilized water present in the center of the reverse micelle. As the water/detergent ratio (w) in the organic bulk solvent increases, the polarity of the solubilized water approaches that of bulk water. However, Blyshak et al.[95] have shown that reverse AOT micelles ([AOT] = 0.10 M) in cyclohexane with $w = 20$ give solubilized water that is still less polar than bulk water. They used ANS as a probe, which displays characteristic bathochromic emis-

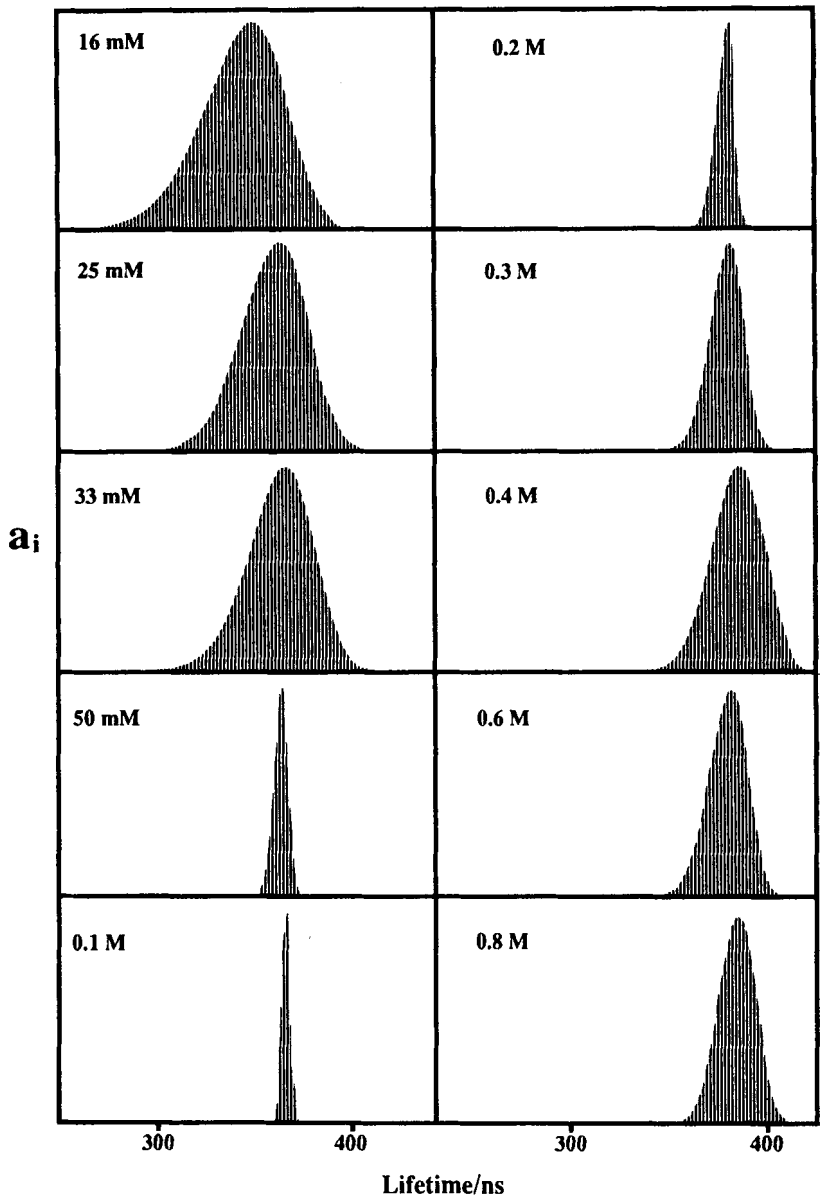

FIGURE 7. Lifetime distributions recovered by MEM from pyrene decays in SDS micelles. [SDS] indicated in the diagrams. (From Siemiarczuk, A.; Ware, W.R. *Chem. Phys. Lett.* **1990,** *167,* 263. With permission.)

sion shifts with decreasing polarity of its immediate surroundings. The ANS emission maximum in the reverse AOT micelles was found at 481 nm, similar to ethylene glycol and well below the 515-nm value in pure water.

An estimate of the radius of the water pool in reverse AOT micelles is provided by the expression[96]

$$R = 36.65v / w_t \qquad (28)$$

where v is the volume/volume percent water, and w_t is the weight/volume percent AOT. Blyshak and Warner[97] have used an AOT/cyclohexane/water reverse micellar system with acetyltrimethylammonium naphthoate as a sensitizing agent (donor) and biphenyl as the phosphorescent

TABLE 3
Refractive Indices (n^{20}_D) of Dioxane-Water Mixtures; Fluorescence Quantum Yields (Φ) and Lifetimes (τ) of Methyl-9-anthroate in These Mixtures at 20°C

$[H_2O]$ (*M*)	n^{20}_D	Φ	τ/n
0	1.4216	0.75	12.8
4.4	1.4200	0.49	8.46
8.8	1.4183	0.36	6.58
13.2	1.4167	0.29	5.18
17.6	1.4148	0.23	4.28
22.0	1.4125	0.18	3.40
26.4	1.4085	0.15	2.86

From Maçanita, A.L.; Costa, F.P.; Costa, S.M.B.; Melo, E.C.; Santos, H. *J. Phys. Chem.* **1989,** *93,* 336. With permission.

acceptor. They note that as the radius of the solubilized water pool calculated with Equation 28 increases beyond 29 Å, the sensitized biphenyl phosphorescence intensity decreases rapidly. They ascribe this to greater fluidity of the headgroup-water interface in reverse micelles as the water content is increased. It leads to greater distances and fewer collisions between donors and acceptors, and hence produces less sensitized phosphorescence from the latter.

It has been determined recently by time-resolved fluorescence and phosphorescence quenching measurements that monodisperse reverse AOT micelles in alkanes form polydisperse clusters.[98] The size of the clusters increases with micelle concentration and chain length of the alkane solvent. Data on this phenomenon are still sparse at this time; but in the systems studied, the number of micelles per cluster varies from approximately 2.5 to 8.5.

Fluorescence quenching in reverse micelles has been used to evaluate the access of quenchers such as molecular oxygen to the micellar water pools. Sáez et al.[99] used large, detergent-like charged probes such as ((1-pyrenyl)butyl) trimethylammonium iodide and monitored the quenching of their fluorescence by oxygen. They found that probes anchored at the micellar surface with the chromophore directed toward the organic mantle of the micelle are quenched by oxygen at a rate that is mainly determined by the solubility and mobility of oxygen in the organic dispersion medium. In contrast, probes that are located such that the chromophore is exposed to the polar micelle interior are quenched at a low rate, indicating that the reverse micelle restricts access of oxygen to the internal water pool of the micelle.

Bimolecular quenching constants obtained with the hydrophilic quenchers fumaronitrile (dynamic) and acrylonitrile (static) in reverse AOT micelles were 1 to 2 orders of magnitude smaller than those obtained in homogeneous ethanol,[100] and their values invariably increased with *w*. In the case of fumaronitrile, this is thought to be due to a decrease in viscosity of the interface; while with acrylonitrile, it is more likely a result of increased polarity of the quencher-probe environment.

Belletête and Durocher and co-workers have published a series of studies in which they used 3H-indole molecules as sensitive probes of microenvironments in surfactant aggregates.[101–107] In an interesting recent development, they have proposed a method of using the fluorescence lifetime of 2-(*p*-dimethylaminophenyl)-3,3-dimethyl-3H-indole in *p*-dioxane/water mixtures as a "polarity ruler" for the measurement of the interfacial dielectric constant of AOT reverse micelles.[108] Despite the fact that this probe has low water solubility and is subject to hydrolysis, its fluorescence lifetime and quantum yield increase when *w* is increased in an AOT/methylcyclohexane/water system. The lifetime data can be fitted to a single exponential decay expression of the form:

$$\tau_0 / \tau = A \exp(-BX_p) + E \qquad (29)$$

where τ_0 is the lifetime in pure *p*-dioxane, X_p is the mole fraction of water added, and A, B, and E are empirical parameters. The nonlinearity parameter, B, in *p*-dioxane/water mixtures is approximately equal to 12 for a good fit with Equation 29, and the same value is applicable to AOT reverse micelles (Figure 8). This indicates that no dielectric enrichment of the probe occurs in the micellar system and that its solvation must be

considered to be similar to that in dioxane/water. The polarity scale obtained from this solvent system can therefore be used to obtain the effective dielectric constant, ε, of the reverse micellar pseudophase. Simple linear relationships between ε and w can be established, such as $\varepsilon = 0.78w + 2.6$ for [AOT] = 0.52 M.

However, Patonay et al.[109] warn that the results of such measurements can be easily misinterpreted because detergents also increase the solubility of hydrophobic fluorophores. The resulting increase in concentration (for instance, drawing material previously adsorbed onto glass surfaces or contained in microcrystallites) may be mistaken for a

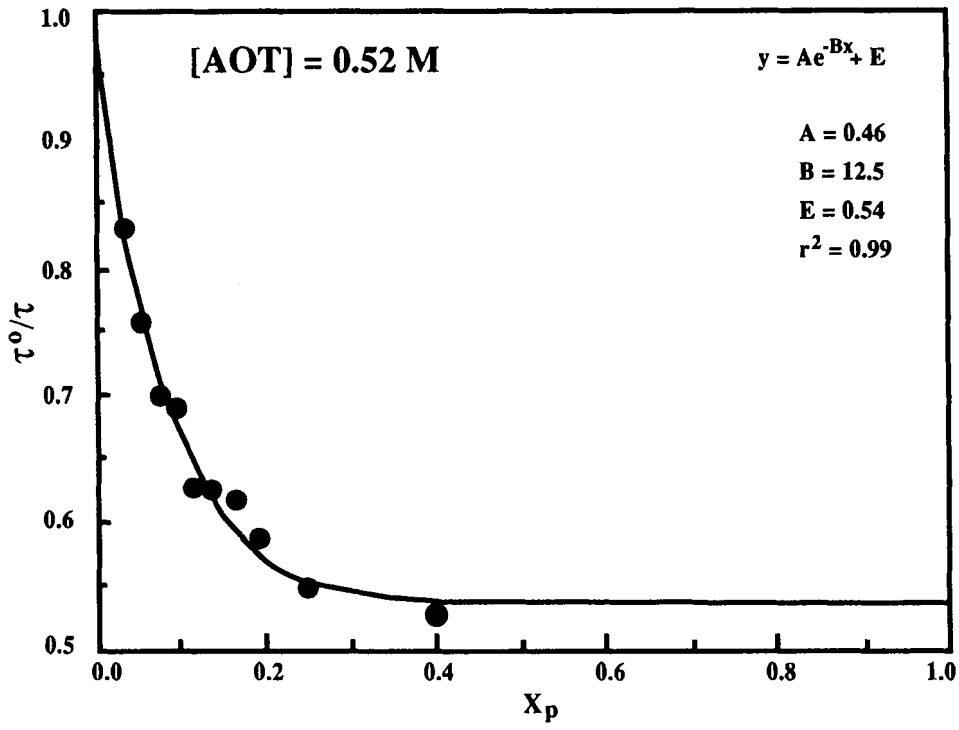

FIGURE 8. Variation of fluorescence lifetime of 2-(*p*-dimethylaminophenyl)-3,3-dimethyl-3H-indole with water mole fraction, X_p. (From Belletête, M.; Durocher, G. *J. Colloid Interface Sci.* **1990,** *134,* 289. With permission.)

Aggregation numbers of reverse micelles are generally smaller than those of comparable normal micelles. The treatment leading to Equation 15 has been used[60] to show that reverse micellar aggregation numbers depend mainly on surfactant concentration, irrespective of w. The numbers for SDS in 1-hexanol/water, for instance, range from 20 to 40, compared to 60 for normal SDS micelles.

F. Fluorescence Enhancement

It is generally accepted that micelles enhance the fluorescence of probes associated with them. more fundamental micellar effect. Results obtained by these authors with pyrene in various micellar solutions show generally modest enhancement factors when increased dissolution is factored out (Table 4). Other studies have shown that it is possible to obtain significant fluorescence enhancement in micellar media.[110,111] The main cause of the enhancement is sequestration of the fluorophore in the micelle and its isolation from quenchers, as well as increased microviscosity of the environment. Tran and Van Fleet[111] have found that intensity enhancement is most pronounced for fluorophores that are structurally similar to the detergent comprising the micelle and therefore

TABLE 4
Relative Fluorescence of Pyrene (3.3×10^{-7} *M*) with Various Micelles

Micelle	Micellar conc. (*M*)	Rel. intensity
None	0	1.00
CTAB	0.0045	0.89–0.78
SDS	0.045	1.44–1.00
SB-12	0.0020	0.97–0.64
TX-100	2.7 vol %	2.02–1.56
CTAC	0.0064	1.59–1.23

From Patonay, G.; Rollie, M.E.; Warner, I.M. *Anal. Chem.* **1985,** *57,* 569. With permission.

TABLE 5
Relative Fluorescence Intensities of Anthracene Derivatives in Different Media

Substrate	Solvent	Φ
Anthracene	Water	1.00
	CTAB	0.95
	CTAC	1.85
	SDS	1.91
	SB-12	2.21
	Brij-35	2.10
	$C_{12}E_6$[a]	2.21
Anthracene propionic acid	Water	1.00
	CTAB	1.53
	CTAC	1.63
	SDS	2.04
	SB-12	2.04
	Brij-35	2.41
	$C_{12}E_6$	2.52
Anthracenepalmitic acid	Water	1.00
	CTAB	2.14
	CTAC	2.23
	SDS	1.62
	SB-12	3.31
	Brij-35	2.99
	$C_{12}E_6$	3.18
Anthracene undecanoic acid	Water	1.00
	CTAB	6.31
	CTAC	6.39
	SDS	2.19
	SB-12	8.37
	Brij-35	10.30
	$C_{12}E_6$	12.22

[a] Hexaethylene glycol mono-*n*-dodecyl ether.

From Tran, C.D.; Van Fleet, T.A. *Anal. Chem.* **1988,** *60,* 2478. With permission.

interact more strongly than others. This is borne out by the data shown in Table 5, where intensities of "detergent-like" fluorophores are most notably enhanced. Ephardt and Fromherz[112] have found that the fluorescence quantum yield of (dibutylamino)stilbazolium butylsulfonate, an amphiphilic dye, increased significantly in micellar detergent solutions, relative to water. The values obtained rivaled those of the fluorophore in very low-polarity organic solvents. In contrast, fluorescence enhancement of 1-naphthol, which has no detergent character, experiences only modest enhancement in various micellar media[33] of selected detergents (Table 6). The fluorescence of porphyrins also shows no more than slight enhancement in micellar solutions.Tetrakis(sulfonatophenyl) porphyrin,[37] for instance, has a quantum efficiency of 0.17 in water, which rises to 0.26 in 0.01 *M* TX-100. In an interesting recent study, Sarkar and Sengupta show that micellar environments can be used to selectively enhance emissions of tautomeric forms of a fluorophore.[28] They used 3-hydroxyflavone, which undergoes excited state proton transfer via an intramolecular hydrogen bond. Its fluorescence emission spectrum displays a blue-violet and a green band. The green emission is strongly enhanced in micellar media, while the blue-violet band is virtually unaffected (Figure 9). This indicates that the green band is due to the proton-transferred tautomer, while the blue-violet band is due to the native molecule. The use of fluorescence anisotropy for the determination of micellar microviscosities was discussed previously in Section C.

G. Chemiluminescence

Chemiluminescence reactions have been used for the determination of biologically important compounds for a considerable length of time,[113] both *in vitro* and *in vivo*. A frequently employed class of enzymatic methods involves the reaction with an oxidase, which produces hydrogen peroxide, and the subsequent quantification of this product. There are several nonenzymatic chemiluminescence (CL) processes that are based on the

TABLE 6
Effect of the Surfactant Nature on the Fluorescence of 1-Naphthol at Neutral pH

Surfactant	Concentration (%)	Rel. intensity
CTAB	0.1	0.23
SDS	1	0.70
SLES	1	1.25
Genapol PF-20	1	1.4
Dehscoxid 728	1	1.78
Triton X-100	1	1.38
Nemol K-1030	1	1.58

From Sancénon, J.; Carrión, J.L.; de la Guardia, M. *Fres. J. Anal. Chem.* **1990,** *336,* 389. With permission.

reaction of the lumiphore with hydrogen peroxide, including those of luminol, lucigenin, acridinium esters, and peroxyoxalates.[114,115] The luminol reaction, for instance, can be effectively used for the determination of cholesterol, amino acids, and glucose in body fluids, involving the typical steps:

$$\beta\text{-D-glucose} + H_2O + O_2 \xrightarrow{\text{glucose oxidase}} \text{gluconic acid} + H_2O_2$$

$$\text{Luminol} + 2\ H_2O_2 + OH^- \xrightarrow{\text{catalyst}} \text{Aminophthalate}^* + N_2 + 3\ H_2O$$

$$\text{Aminophthalate}^* \longrightarrow \text{Aminophthalate} + h\nu$$

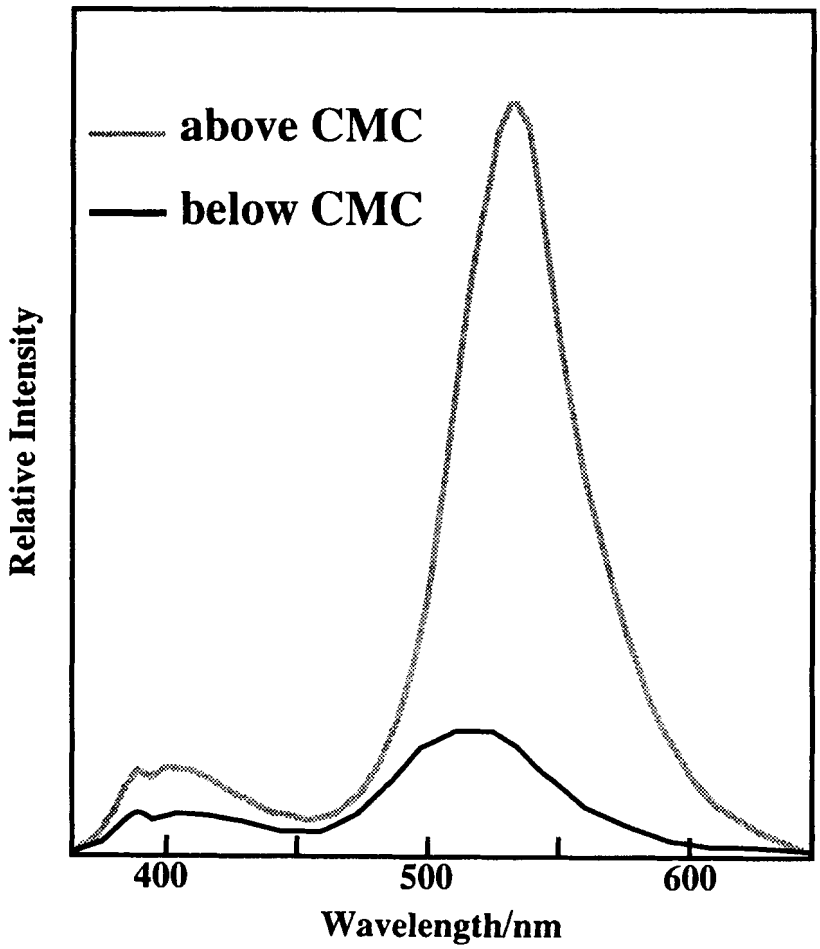

FIGURE 9. Emission spectra of 3-hydroxyflavone (2×10^{-5} *M*) in Triton X-100 solutions. (From Sarkar, M.; Sengupta, P.K. *Chem. Phys. Lett.* **1991,** *179,* 68. With permission.)

A serious problem encountered with analytically useful CL reactions that follow enzymatic production of peroxide is the pH mismatch inherent in these systems. A case in point is again the luminol reaction, which requires an alkaline solution (pH ~ 11). In contrast, the oxidase reaction preceding it in the process can only tolerate a pH in the range 7 to 8.5. The use of micellar solutions avoids the need for separate bulk media to conduct the two stages of the reaction.[116–118] Cetyltrimethylammonium bromide (CTAB) micelles have been found to give six- sevenfold enhanced luminol CL signals compared to solutions without surfactant,[119] while other cationic and nonionic surfactants gave lesser enhancements. The bulk of the solution was buffered at pH 7.25, the ideal conditions for the action of glucose oxidase. A limit of detection of 1×10^{-7} *M* glucose was obtained, and no catalyst was required for the luminol reaction.

Reverse micelles have also been successfully employed for the luminol reaction,[120,121] using, for instance, a chloroform-cyclohexane mixed bulk solvent and CTAB detergent. The reaction conditions have been carefully described by Hoshino and Hinze[119] in a paper that details all important parameters. In a later paper,[120] glucose was determined with a 2.7×10^{-8} *M* detection limit. It should be noted that all relevant reactions are taken to occur in the reversed micellar microreactor, without explicit involvement of the organic phase. The evident relaxation of pH requirements for the different reactions in the micellar interior has been noted and analytically exploited, but never mechanistically explained.

H. Phosphorescence

Phosphorescence is the radiative conversion of a triplet excited state of an emitting species to a singlet ground state. It can only be observed if the surroundings of the phosphor are such that collisional deactivation and vibrational relaxation are sufficiently reduced during the excited-state lifetime, which can range from microseconds to seconds. Traditionally, there have been two ways of achieving the required environmental rigidity: with a frozen (77 K) matrix or through strong surface adsorption. Phosphorescence in fluid solutions can be observed under certain circumstances involving thorough removal of dissolved oxygen and the use of unreactive solvents such as perfluorocarbons. Micelle-stabilized room-temperature phosphorescence (MS-RTP) provides a more widely applicable method of generating phosphorescence emission, while it eliminates the experimental complications inherent in cryogenic or adsorptive procedures.

MS-RTP was first reported by Kalyanasundaram et al.[122] and subsequently elaborated by other workers.[123–127]. A brief review has been presented by Cline Love and Skrilec.[128] Micellar media provide a number of features that can promote RTP of phosphors solubilized in the nonpolar micellar interior. First, the structured nature of this microenvironment minimizes collisional deactivation of excited species by restricting their diffusive motions. Second, exclusion of quenchers from the interior of the micelle through polarity considerations reduces the probability of other quenching encounters. Reduction of interactions with oxygen are particularly germane, allowing for MS-RTP in some solutions that have not been deaerated. A third extremely important possibility provided by micellar solutions concerns the effective inclusion of heavy atoms. It is well known that the heavy atom effect strongly promotes phosphorescence by facilitating intersystem crossing.[9] The counter cation of anionic detergents such as SDS can be replaced easily by a heavy element like thallium or silver. The intrinsic proximity between the fluorescent probe enclosed in the micelle and the counterions of the detergent making up the micelle results in a pronounced heavy atom effect and increased phosphorescence. Figure 10 shows the phosphorescence of naphthalene in a 77-K ethanol glass and in a room-temperature micellar SDS solution containing thallium. The similarity of the emissions in the two cases is evident. Limits of detection and other analytical figures of merit obtained with MS-RTP are comparable to those found with low-temperature phosphorescence.

Sanz-Medel and co-workers have shown that MS-RTP can be significantly enhanced by chemical deoxygenation with sodium sulfite[129] and that it can be utilized for the determination of metals.[130] This was demonstrated with a series of phosphorescent niobium(V)-hydroxyquinoline

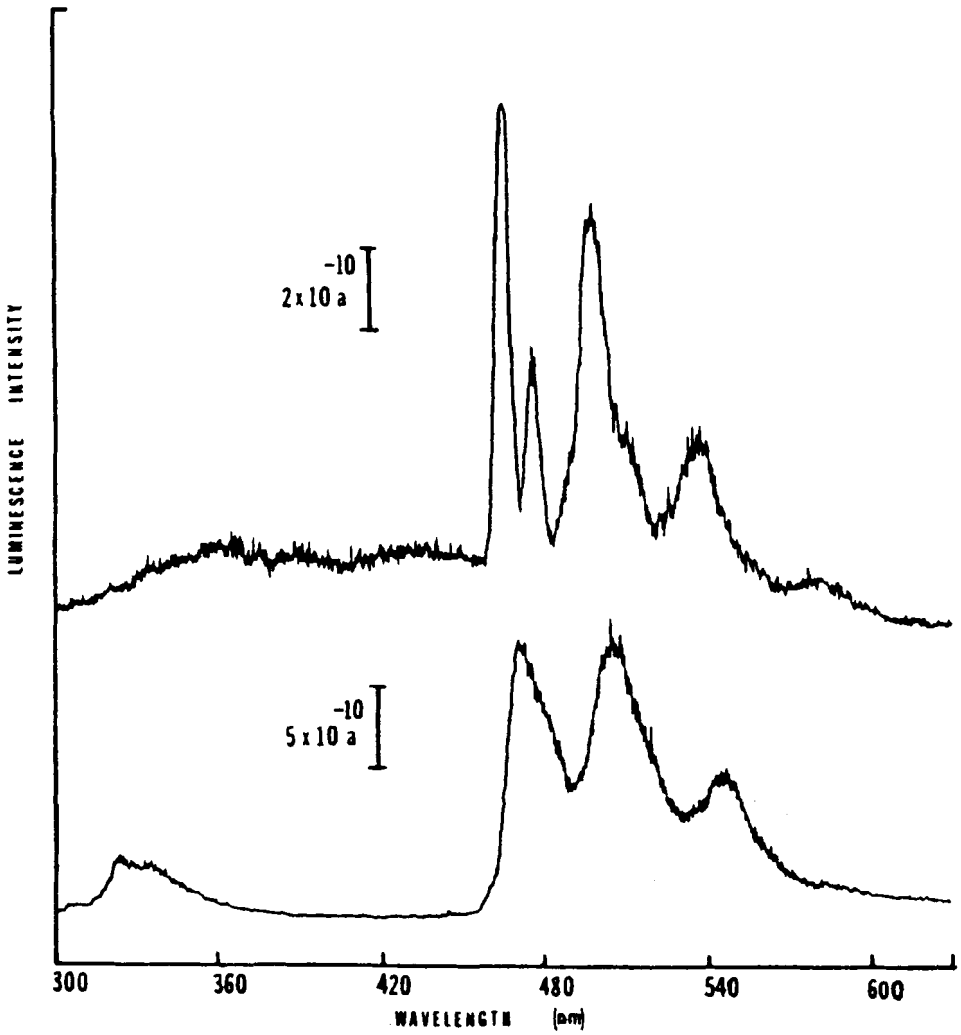

FIGURE 10. Luminescence spectra of 6×10^{-5} *M* naphthalene in ethanol at 77 K (upper trace) and in 0.15 *M* TILS/NaLS micellar system with 30% Tl^+ at room temperature (lower trace). (From Cline Love, L.J.; Skrilec, M.; Habarta, J.G. *Anal. Chem.* **1980,** *52,* 754. With permission.)

complexes isolated in CTAB, Brij-35, and SDS micelles. It was noted that additional external heavy atoms were required for useful RTP signals in all cases and that small haloalkanes such as Br_3CH were most suitable for this purpose.

The use of detergents in paper-substrate room-temperature phosphorescence has also been studied and found to have notable beneficial effects.[131] Signal enhancements in the two- to ninefold range were encountered for PAHs adsorbed on filter paper and brought in contact with SDS containing Tl^+. In the sorptive interactions operative in this process, true micelles as found in single-macrophase solutions cannot be present at the surface. It is proposed that the enhancement is caused by improved heavy atom-phosphor proximity, and by increased migration of the species into the cellulose pores of the paper.

The quenching of MS-RTP has been found to increase with quencher concentration until a plateau is reached.[132] This is true for phosphors that are virtually exclusively present inside the micelles, and is therefore indicative of a quenching process that takes place at the micellar surface. This would lead to the observed quenching behavior because, with a fixed micelle concentra-

tion, the surface area (and hence the quenching interactions) would be limited, resulting in concomitantly limited quenching.

Kim et al.[133] have recently investigated the effects of environmental factors on MS-RTP lifetimes. They present a convenient kinetic model for MS-RTP, in which for the first time account is taken of the external heavy atom effect (Figure 11A). Increasing the temperature was found to decrease both intensity and lifetime in MS-RTP (Table 7), while an increase in heavy atom concentration decreased the lifetime but increased the intensity. When the data in Figure 11 are plotted as k_o (decay rate constant) vs. $[Tl^+]$, a straight line is obtained. This effect is not fully understood at present, although the observations can be rationally represented by[132]

$$\frac{1}{\tau} = k_0 = k_- + k_{mp} + k_{mh}[H] + k' - \left\{ \frac{k_+ k_- [M]}{k_+ [M] + k_h [H] + k''} \right\} \quad (30)$$

where τ is the phosphorescence lifetime, [H] is the heavy atom concentration, [M] is the micelle concentration, $k' = k_{mq}[Q]$ and $k'' = k_q[Q]$. All other symbols are defined in Figure 11. At a fixed value of [M] in a system, k_0 depends mostly on $k_{mh}[H]$ and $k_h[H]$. Furthermore, because of the opposite charges of the heavy atom and the micelle, it is expected that $k_{mq} >> k_h$. The rate constant k_0 is therefore a roughly linear function of $k_{mh}[H]$. In physical terms, heavy atoms increase the rate constants of both decay transitions involved in the phosphorescence process (S_1 - T_1, and T_1 - S_0), and therefore reduce the phosphorescence lifetime.[134]

I. Metals

Metals may be used in micellar luminescence studies as quenchers or, in the form of complexes, as fluorophores. Both roles provide some opportunity for analysis of metals, but more commonly they are used to probe the micellar environment or mechanistic pathways therein.

Fluorescence of the ubiquitous probe pyrene, for instance, is quenched in SDS micelles by Cu^{2+}, Tl^+, Hg^{2+}, Eu^{3+}, Ag^+, Ni^+, Mn^{2+} Sm^{3+}, Cs^+, and Co^{2+}. The mechanism of quenching by Cu^{2+} and Co^{2+} has been used[135] to study the location of pyrene within the micelle. It was found that both metals quench micellized pyrene strongly, producing nonexponential decay curves at all metal concentrations. At low (<0.005 *M*) quencher concentration, the fluorescence intensity was effectively quenched, but the I_1/I_3 ratio of the emission did not change. At quencher concentrations, >0.005 *M*, I_1/I_3 decreased as quencher concentration increased, indicating that pyrene experiences a less polar environment at the higher metal concentrations. An additional consideration of lighter metal ions revealed that the quenching effect of the metal does not correlate with its influence on I_1/I_3. The conclusion was reached that pyrene resides near the surface of the micelle and is accessible to quenching by solution-borne metal ions. The influence of high metal ion concentration on I_1/I_3 can be interpreted in more than one way. The most probable explanation appears to be that at high quencher/electrolyte concentrations, the micellar aggregation number increases, the micelle "tightens up," and water penetration decreases.

The location of the metal-based fluorophore $Ru(bpy)_3^{2+}$ in SDS micelles has been the subject of investigation for a number of years, and it is generally agreed that both hydrophobic and electrostatic factors play a role.[136–139] In a recent study,[140] a series of doxylstearic acids were used as fluorescence quenchers. These are long, detergent-like free radical species (Figure 12) that comicellize with SDS. The doxyl group is the quenching chromophore and its point of attachment to the hydrocarbon backbone (5-, 7-, 12-, or 16-position) determines how well a $Ru(bpy)_3^{2+}$ ion located at some preferred place along this chain is quenched. The quenching order in the micelle is 7-D > 5-D > 12-D > 16-D, which leads to the conclusion that the probe is located as illustrated in Figure 12.

Direct determination of metals by micellar fluorescence has focused on niobium and tantalum through a variety of complexes.[141–143] Cationic and nonionic detergents were found to give

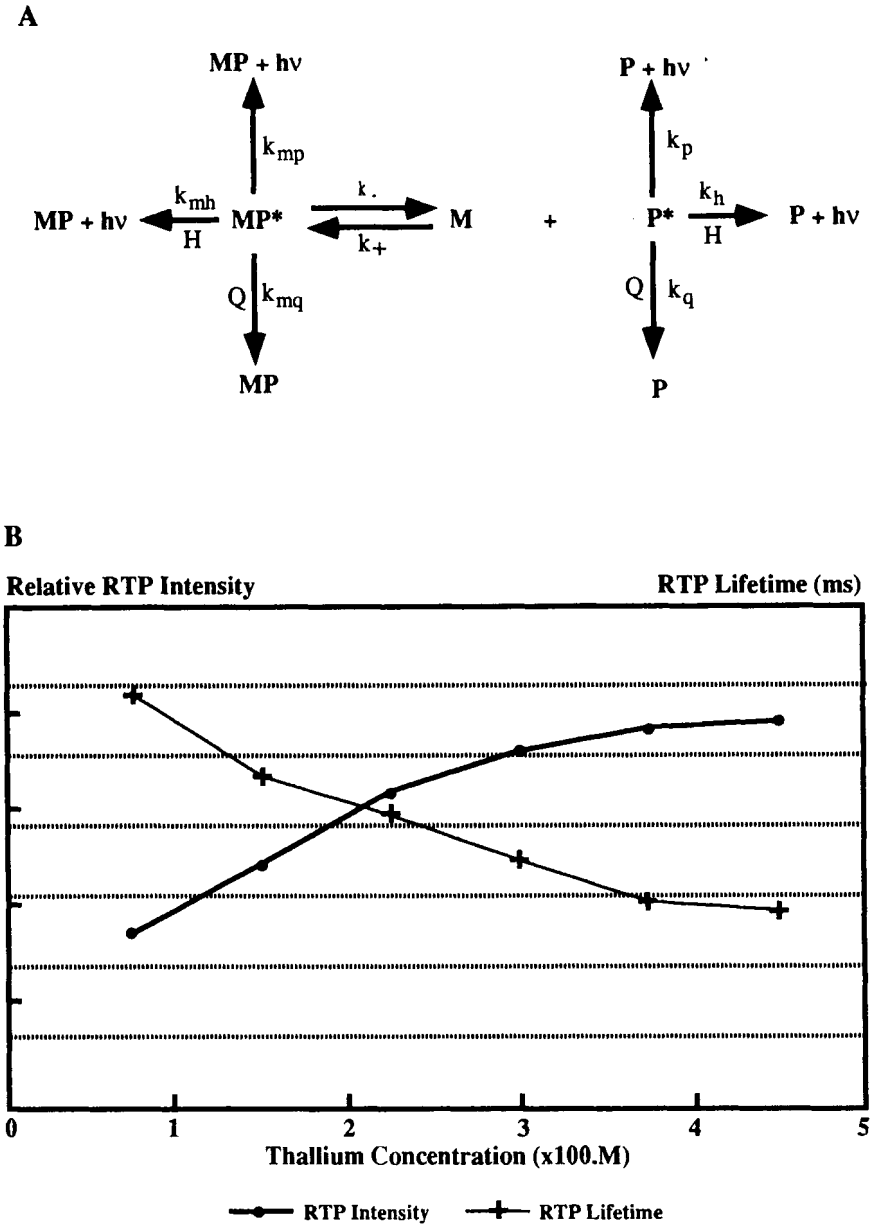

FIGURE 11. (A) Kinetic model of MS-RTP: M, micelle; P, triplet probe; Q, quencher; H, heavy atom; MP* represents the excited triplet probe located inside the micelle and the rate constants are defined as indicated by the arrows. (B) Heavy atom (Tl^+) effect on MS-RTP intensity and MS-RTP lifetime of pyrene: [pyrene] = 5×10^{-5} M, [SDS] = 0.05 *M*, [SO_3^{2-}] = 0.02 *M*. (From Kim, H.; Crouch, S.R.; Zabik, M.J.; Selim, S.A. Anal. Chem. 1990, 62, 2365. With permission.)

fluorescence enhancement, but anionic SLS did not since the metal complexes studied were negatively charged and therefore repelled by anionic micelles. As complexing agents, flavonols gave the best results, especially morin, and mostly so in cationic micelles of CPB and CTAB. Detection limits of 1 ppb for niobium and 30 ppb for tantalum were obtained. Lumogallion complexes of niobium gave good fluorescence enhancement in a series of nonionic detergents, especially of the

TABLE 7
Effect of Temperature on RTP of Pyrene

Temperature (°C)	RTP Intensity	RTP lifetime (ms)
15	656	6.02
20	590	5.36
25	532	5.02
30	502	4.93
35	468	4.89

From Kim, H.; Crouch, S.R.; Zabik, M.J.; Selim, S.A. *Anal. Chem.* **1990,** *62,* 2365. With permission.

Triton and Nemol series. Auxilliary ligands such as tartrate, oxalate, or citrate were necessary to produce this effect, and the optimal pH was 1.

The fluorescence properties of 8-hydroxyquinoline-5-sulfonic acid complexes of 42 metals have been reported[144] and it was noted that tenfold emission enhancements could be obtained for some of these in HTAC micelles. The metals studied in micellar environments were Mg, Sr, Ba, Al, Zn, and Cd, with Al giving the greatest enhancement (10.2 times).

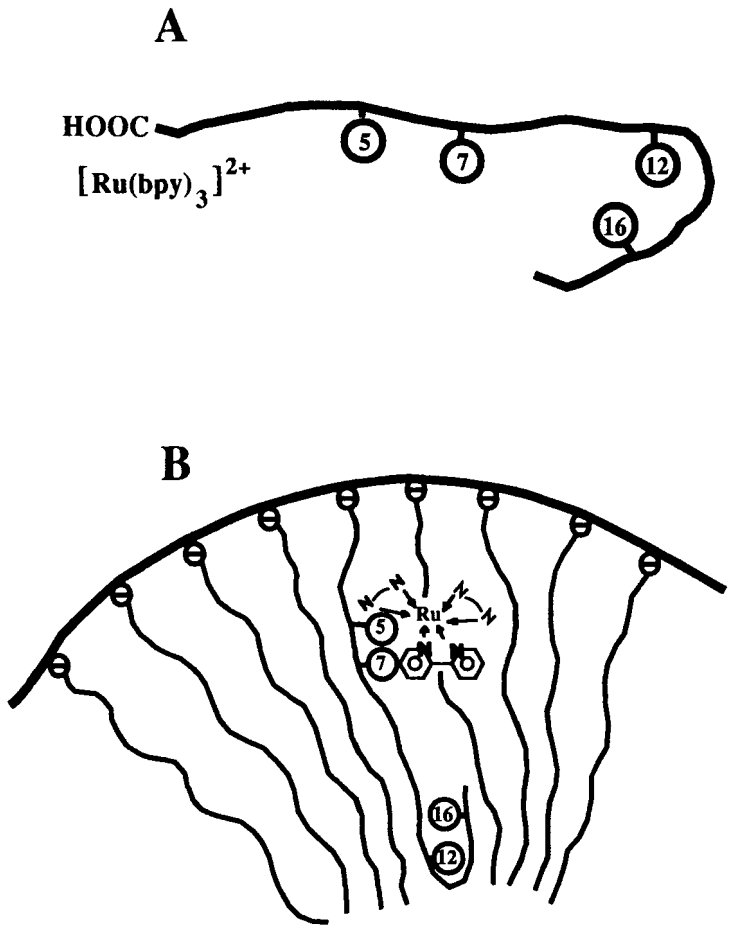

FIGURE 12. Representations of doxylstearic acid molecule and $Ru(bpy)_3^{2+}$ in water (A), and both species in an SDS micelle (B). (From Kunjappu, J.T.; Somasundaran, P.; Turro, N.J. *J. Phys. Chem.* **1990,** *94,* 8464. With permission.)

IV. CONCLUSIONS

The micellar pseudophase continues to hold fascination for chemists and physicists with many varied interests, and luminescence spectroscopy will unquestionably play a major role in future advances in the field. As the fundamental knowledge of detergent micelles and related aggregates increases, analytical chemists will continue to reap benefits in the form of improved methodology and analytical performance of luminescence techniques.

While the entire field of luminescence spectroscopy in micellar media is a fertile one for researchers, some areas deserve special attention. Included in these is the role of micelles in chemiluminescence and the question of their benefits in matching solution conditions to different stages of the reaction sequence. These benefits have clearly been shown to exist, but the mechanisms are not well understood at this time. Another field requiring further study is MS-RTP, especially with the external heavy atom effect, where the influence of temperature remains somewhat unclear. The relation of metal ions to micellized pyrene and their relative positions in (or on) detergent aggregates also needs to be further investigated. The Ham effect of pyrene is the key to this study.

The phenomenon of clouding in nonionic detergent solutions is interesting from both fundamental and practical standpoints. Studies are presently being carried out in the author's laboratory on the structure of the detergent phase and the kinetics of its formation. The use of cloud point separation for large-scale extractions relevant to pollution remediation is also under investigation.

The new and exciting field of micellar chromatography is beyond the scope of this review, but it should be noted that fluorescence detection, both through on- and post-column mechanisms, is eminently suited for this type of chromatography. The field is wide open for further development and research into new methodology should be encouraged.

REFERENCES

1. Mittal, K.L.; *Micellization, Solubilization, and Microemulsions,* Vols. 1 & 2; Plenum Press; New York, **1977**.
2. Kalyanasundaram, K. *Chem. Soc. Rev.* **1978**, *7*, 453.
3. Thomas, J.K. *Acc. Chem. Res.*, **1977**, *10*, 133.
4. Turro, N.J.; Grätzel, M.; Braun, A.M. *Angew. Chem. Int. Ed. Engl.* **1980**, *19*, 675.
5. Hinze, W.L.; Singh, H.N.; Baba, Y.; Harvey, N.G. *Trends Anal. Chem.* **1984**, *3*, 193.
6. Grieser, F.; Drummond, C.J. *J. Phys. Chem.* **1988**, *92*, 5580.
7. Georges, J. *Spectrochim. Acta Rev.* **1990**, *13*, 27.
8. McIntire, G.L. *Crit. Rev. Anal. Chem.* **1990**, *21*, 257.
9. Lakowicz, J.R.; *Principles of Fluorescence Spectroscopy;* Plenum Press: New York, 1983.
10. *Molecular Luminescence Spectroscopy,* Parts I & II; Schulman, S.G. Ed.; John Wiley & Sons: New York, 1988.
11. *Practical Fluorescence;* 2nd ed.; Guilbault, G.G. Ed.; Marcel Dekker: New York, 1990.
12. *Topics in Fluorescence Spectroscopy;* Vols. 1–3; Lakowicz, J.R. Ed.; Plenum Press: New York, 1991.
13. *Luminescence Applications,* Goldberg, M.C. Ed.; ACS Symposium Series 383, American Chemical Society, Washington, D.C., 1989.
14. Kalyanasundaram, K.; Thomas, J.K. *J. Am. Chem. Soc.* **1977**, *99*, 2039.
15. Nakajima, A. *Bull. Chem. Soc. Jpn.* **1971**, *44*, 3272.
16. Nakajima, A. *Spectrochim. Acta, Part A.* **1974**, *30*, 860.
17. Weber, G.; Teale, F.W.J. *Trans Faraday Soc.* **1957**, *53*, 646.
18. Sawicki, E.; Hauser, T.R.; Stanley, T.W. *Int. J. Air Pollut.* **1960**, *2*, 253.
19. Melo, E.C.C.; Costa, S.M.B. *J. Chem. Soc. Faraday Trans.* **1990**, *86*, 2155.
20. Siemiarczuk, A.; Koput, J.; Pohorille, A. *Z. Naturforsch.* **1982**, *37a*, 598.
21. Parker, C.A.; *Photoluminescence of Solutions;* Elsevier: New York, 1968; Chapter 5.
22. Parker, C.A.; Hatchard, C.G.; Joyce, T.A. *J. Mol. Spectrosc.* **1964**, *14*, 311.
23. Parker, C.A.; Hatchard, C.G. *Analyst.* **1962**, *87*, 644.
24. Parthasarathy, R.; Labes, M.M. *Langmuir.* **1990**, *6*, 542.
25. Wehry, E.L.; *Practical Fluorescence;* 2nd ed., Guilbault, G.G. Ed.; Marcel Dekker: New York, 1990; pp. 81.
26. Ephardt, H.; Fromherz, P. *J. Phys. Chem.* **1989**, *93*, 7717.

27. Jobe, D.J.; Verrall, R.E. *Langmuir.* **1990,** *6,* 1750.
28. Sarkar, M.; Sengupta, P.K. *Chem. Phys. Lett.* **1991,** *179,* 68.
29. Maçanita, A.L.; Costa, F.P.; Costa, S.M.B.; Melo, E.C.; Santos, H. *J. Phys. Chem.* **1989,** *93,* 336.
30. Reekmans, S.; Luo, H.; van der Auweraer, M.; de Schryver, F.C. *Langmuir.* **1990,** *6,* 628.
31. Brochsztain, S.; Filho, P.B.; Toscano, V.G.; Chaimovich, H.; Politi, M.J. *J. Phys. Chem.* **1990,** *94,* 6781.
32. Hofstraat, J.W.; Gooijer, C.; Velthorst, N.H. *Molecular Luminescence Spectroscopy,* Part 2; Schulman, S.G. Ed.; John Wiley & Sons: New York, 1988; pp. 335.
33. Sancénon, J.; Carrión, J.L., de la Guardia, M. *Fresenius' J. Anal. Chem.* **1990,** *336,* 389.
34. Berlman, I.B. *Handbook of Fluorescence Spectra of Aromatic Molecules*; 2nd ed., Academic Press: New York, 1971.
35. Ananthapadmanabhan, K.P.; Goddard, E.D.; Turro, N.J.; Kuo, P.L. *Langmuir.* **1985,** *1,* 352.
36. Parker, C.A. *Proc. R. Soc. (London) A.* **1963,** *276,* 125.
37. Basu, S. *J. Photochem. Photobiol. A: Chem.* **1991,** *56,* 339.
38. Joshi, V.; Gosh, P.K. *J. Am. Chem. Soc.* **1989,** *111,* 5604.
39. Stryer, L. *Annu. Rev. Biochem.* **1978,** *47,* 819.
40. Dale, R.E.; Eisinger, J. *Biopolymers.* **1974,** *13,* 1573.
41. Lowey, S.; Marsh, D.J. *Biochemistry.* **1980,** *19,* 774.
42. Armstrong, D.W.; Spino, L.A.; Ondrias, M.R.; Findsen, E.W. *J. Am. Chem. Soc.* **1986,** *108,* 5646.
43. Spino, L.A.; Armstrong, D.W.; Alak, A.M.; Vo-Dinh, T. *Appl. Spectroscopy.* **1987,** *41(5),* 771.
44. Myers, D. *Surfactant Science and Technology,* VCH Publishers: Weinheim, Germany, 1988.
45. Shaw, D.J.; *Introduction to Colloid and Surface Chemistry;* 3rd ed., Butterworths: London, 1980.
46. *Ordered Media in Chemical Separations,* Hinze, W.L.; Armstrong, D.W. Eds.; ACS Symposium Series, American Chemical Society, Washington, D.C., 1987.
47. Prince, L.M., *J. Colloid Interface. Sci.* **1975,** *52,* 182.
48. Shah, D.O.; Bansal, V.K.; Chan, K.; Hsieh, W.C. *Improved Oil Recovery by Surfactant and Polymer Flooding;* Shah, D.O.; Schechter, R.S. Eds.; Academic Press: New York, 1977.
49. Turro, N.J.; Okubo, T. *J. Am. Chem. Soc.* **1981,** *103,* 7224.
50. Turro, N.J.; Aikawa, M.; Yekta, A. *J. Am. Chem. Soc.* **1979,** *101,* 772.
51. Yekta, A.; Aikawa, M.; Turro, N.J. *Chem. Phys. Lett.* **1979,** *63,* 543.
52. Atik, S.S.; Thomas, J.K. *J. Am. Chem. Soc.* **1981,** *103,* 3543.
53. Khalil, O.S.; Sonnessa, A.J. *Mol. Photochem.* **1977,** *8,* 399.
54. Ndou, T.T.; von Wandruszka, R. *Anal. Lett.* **1988,** *21(11),* 2091.
55. Mukerjee, P.; Mysels, K.J. National Standardized Reference Data Service of the National Bureau of Standards, No. 36.15, 1971.
56. Wilhelm, M.; Zjao, Z.-L.; Wang, Y.; Xu, R.; Winnik, M. *Macromolecules.* **1991,** *24,* 1033.
57. Turro, N.J.; Yekta, A. *J. Am. Chem. Soc.* **1978,** *78,* 5951.
58. Almgren, M.; Löfroth, J.-E. *J. Colloid Interface Sci.* **1980,** *81,* 486s.
59. Rodgers, M.A.; Baxendale, J.H. *Chem. Phys. Lett.* **1981,** *81,* 347.
60. Rodenas, E.; Pérez-Benito, E. *J. Phys. Chem.* **1991,** *95,* 4552.
61. Grieser, F.; Drummond, C.J. *J. Phys. Chem.* **1988,** *92,* 5580.
62. Infelta, P.P.; Grätzel, M.; Thomas, J.K. *J. Phys. Chem.* **1974,** *78,* 190.
63. Almgren, M.; Löfroth, J.E. *J. Chem Phys.* **1982,** *76,* 2734.
64. Warr, G.G.; Grieser, F.J. *J. Chem. Soc. Faraday Trans. 1.* **1986,** *82,* 1813.
65. Lang, J. *J. Phys. Chem.* **1990,** *94,* 3734.
66. Reekmans, S.R.; Luo, H.; van der Auweraer, M.; de Schryver, F.C. *Langmuir.* **1990,** *6,* 628.
67. Atik, S.S.; Nam, M.; Singer, L.A. *Chem. Phys. Lett.* **1979,** *67(1),* 75.
68. Lianos, P.; Zana, R. *J. Phys. Chem.* **1980,** *84,* 3339.
69. Cogan, U.; Shinitzky, M.; Weber, G.; Nishida, T. *Biochemistry.* **1973,** *12(3),* 521.
70. Shinitzky, M.; Barenholz, Y. *J. Biol. Chem.* **1974,** *249,* 2652.
71. Dale, R.E.; Chen, L.A.; Brand, L. *J. Biol. Chem.* **1977,** *252,* 7500.
72. Chen, L.A.; Dale, R.E.; Roth, S.; Brand, L. *J. Biol. Chem.* **1977,** *252,* 2163.
73. Zachariasse, K. *Chem. Phys. Lett.* **1978,** *57,* 429.
74. Melnick, R.L.; Haspel, H.C.; Goldenberg, M.; Greenbaum, L.M.; Weinstein, S. *Biophys. J.* **1981,** *34,* 499.
75. Lianos, P.; Lang, J.; Strazielle, C.; Zana, R. *J. Phys. Chem.* **1982,** *86,* 1019.
76. Lianos, P.; Viriot, M.L.; Zana, R.J. *J. Phys. Chem.* **1984,** *88,* 1098.
77. Anderson V.C.; Weiss, R.G. *J. Am. Chem. Soc.* **1984,** *106,* 6628.
78. Wirth, M.J.; Chou, S.-H.; Piasecki, D.A. *Anal. Chem.* **1991,** *63,* 146.
79. Chou, S.-H.; Wirth, M.J. *J. Phys. Chem.* **1989,** *93,* 7694.
80. Zwanzig, R. *J. Chem. Phys.* **1970,** *52(7),* 3625.
81. Perrin, F. *J. Phys. Radium.* **1936,** *7,* 1.
82. Hu, C.-M.; Zwanzig, R. *J. Chem. Phys.* **1974,** *60,* 4354.

83. Youngren, G.K.; Acrivos, A. *J. Chem. Phys.* **1975,** *63,* 3846.
84. Chuang, T.J.; Eisenthal, K.B. *J. Chem. Phys.* **1972,** *57,* 5094.
85. Choi, K.-J.; Turkevich, L.A.; Loza, R. *J. Phys. Chem.*, **1988,** *92,* 2248.
86. Förster, Th. *Ann. Phys. (Leipzig).* **1948,** *2,* 55.
87. Kasatani, K.; Kawasaki, M.; Sato, H.; Nakashima, N. *J. Phys. Chem.* **1985,** *89,* 545.
88. Mazer, N.; Benedek, G.; Carey, M.C. *J. Phys. Chem.* **1976,** *80,* 1075.
89. Almgren, M.; Alsins, J.; Mukhtar, E.; van Stam, J. *J. Phys. Chem.* **1988,** *92,* 4479.
90. Alsins, J.; Almgren, M. *J. Phys. Chem.* **1990,** *94,* 3062.
91. Gull, S.F.; Daniell, G.J. *Nature.* **1978,** *272,* 686.
92. Livesey, A.K.; Brochon, J.C. *Biophys. J.* **1987,** *52,* 693.
93. Siemiarczuk, A.; Ware, W.R. *Chem. Phys. Lett.* **1989,** *160,* 285.
94. Siemiarczuk, A.; Ware, W.R. *Chem. Phys. Lett.* **1990,** 167, 263.
95. Blyshak, L.A.; Rollie-Taylor, M.; Sylvester, D.W.; Underwood, A.L.; Patonay, G.; Warner, I.M. *J. Colloid Interface. Sci.* **1990,** *136,* 509.
96. Wong, M.; Thomas, J.K.; Nowak, T. *J. Am. Chem. Soc.* **1977,** *99,* 4730.
97. Blyshak, L.A.; Warner, I.M. *Anal. Chem.* **1990,** *62,* 1953.
98. Jóhannsson, R.; Almgren, M.; Alsins, J. *J. Phys. Chem.* **1991,** *95,* 3819.
99. Sáez, M.; Abui, A.; Lissi, E.A. *Langmuir.* **1989,** *5,* 942.
100. Encinas, M.V.; Lissi, E.A.; Previtali, C.M.; Cosa, J. *Langmuir.* **1989,** *5,* 805.
101. Belletête, M.; Durocher, G. *J. Photochem.* **1983,** *21,* 251.
102. Belletête, M.; Lessard, G.; Richer, J.; Durocher, G. *J. Luminescence.* **1986,** *34,* 279.
103. Belletête, M., Lessard, G.; Durocher, G. *Can. J. Spectrosc.* **1986,** *31,* 89.
104. Richer, J.; Lessard, G.; Belletête, M.; Durocher, G. *Int. J. Chem. Kin.,* **1986,** *18,* 1163.
105. Belletête, M.; Durocher, G. *J. Photochem. Photobiol. A: Chem.* **1988,** *44,* 275.
106. Belletête, M.; Durocher, G. *J. Phys. Chem.* **1989,** *93,* 1793.
107. Belletête, M.; Lessard, G.; Durocher, G. *J. Luminescence.* **1989,** *42,* 337.
108. Belletête, M.; Durocher, G. *J. Colloid Interface Sci.* **1990,** *134,* 289.
109. Patonay, G.; Rollie, M.E.; Warner, I.M. *Anal. Chem.* **1985,** *57,* 569.
110. Kalyanasundaram, K.; *Photochemistry in Microheterogeneous Systems,* Academic Press: Orlando, FL, 1987; pp. 36.
111. Tran, C.D.; Van Fleet, T.A. *Anal. Chem.* **1988,** *60,* 2478.
112. Ephardt, H.; Fromherz, P. *J. Phys. Chem.*, **1989,** *93,* 7717.
113. *Methods of Enzymatic Analysis;* Volkert, E.; Bergmeyer, H.V. Eds.; Vol. 1; Verlag Chemie: Deerfield Beach, FL, 1983; pp. 261.
114. Seitz, W.R. *Crit. Rev. Anal. Chem.* **1981,** *13,* 1.
115. Grayeski, M.L., *Anal. Chem.* **1987,** *59(21),* 1243A.
116. Kamidate, T.; Yoshida, K.; Kaneyasu, T.; Sagawa, T.; Watanabe, H. *Anal. Sci.* **1990,** *6,* 645.
117. Hinze, W.L.; Riehl, T.A.; Singh, H.N.; Baba, Y. *Anal. Chem.* **1984,** *56,* 2180.
118. Malehorn, C.L.; Riehl, T.A.; Hinze, W.L. *Analyst.* **1986,** *111,* 941.
119. Abdel-Latif, M.S.; Guilbault, G.G. *Anal. Chim. Acta.* **1989,** *221,* 11.
120. Hoshino, H.; Hinze, W.L. *Anal. Chem.* **1987,** *59,* 496.
121. Igarashi, S.; Hinze, W.L. *Anal. Chim. Acta,* **1989,** *225,* 147.
122. Kalyanasundaram, K.; Grieser, F.; Thomas, J.K. *Chem. Phys. Lett.*, **1977,** *51,* 501.
123. Almgren, M.; Grieser, F.; Thomas, J.K. *J. Am. Chem. Soc.* **1979,** *101,* 279.
124. Turro, N.J.; Liu, K.C.; Chow, M.F.; Lee, P. *Photochem. Photobiol.* **1978,** *27,* 523.
125. Cline Love, L.J.; Skrilec, M.; Habarta, J.G. *Anal. Chem.* **1980,** *52,* 754.
126. Scypinski, S.; Cline Love, L.J. *Anal. Chem.* **1984,** *56,* 322.
127. Femia, R.A.; Cline Love, L.J. *Anal. Chem.* **1984,** *56,* 327.
128. Cline Love, L.J.; Skrilec, M. *Am. Lab.* **1981,** *March,* 103.
129. Díaz García, M.E.; Sanz-Medel, A. *Anal. Chem.* **1986,** *58,* 1436.
130. Sanz-Medel, A.; Martinez Garcia, P.L.; Díaz García, M.E. *Anal. Chem.* **1987,** *59,* 774.
131. Ramis Ramos, G.; Garcia Alvarez-Coque, M.C.; O'Reilly, A.M.; Khasawneh, I.M.; Winefordner, J.D. *Anal. Chem.* **1988,** *60,* 416.
132. Bolt, J.D.; Turro, N.J. *J. Phys. Chem.* **1981,** *85,* 4029.
133. Kim, H.; Crouch, S.R.; Zabik, M.J.; Selim, S.A. *Anal. Chem.* **1990,** *62,* 2365.
134. Humphry-Baker, K.R.; Moroi, Y.; Graetzel, M. *Chem. Phys. Lett.* **1978,** *58,* 207.
135. Konuk, R.; Cornelisse, J.; McGlynn, S.P. *J. Phys. Chem.* **1989,** *93,* 7405.
136. Meisel, D.; Matheson, M.S.; Rabani, J. *J. Am. Chem. Soc.* **1978,** *100,* 117.
137. Warr, G.G.; Grieser, F. *Chem. Phys. Lett.* **1985,** *116,* 505.
138. Hauenstein, B.L., Jr.; Dressick, W.J.; Buell, S.I.; Demas, J.N.; Degraff, B.A. *J. Am. Chem. Soc.* **1983,** *105,* 4251.
139. Colaneri, M.J.; Kevan, L.; Schmehl, R. *J. Phys. Chem.* **1989,** *93,* 397.

140. Kunjappu, J.T.; Somasundaran, P.; Turro, N.J. *J. Phys. Chem.* **1990,** *94,* 8464.
141. Sanz-Medel, A.; Garcia Alonzo, J.I. *Anal. Chim. Acta.* **1984,** *165,* 159.
142. Sanz-Medel, A.; Garcia Alonso, J.I.; Blanco González, E. *Anal. Chem.* **1985,** *57,* 1681.
143. Sanz-Medel, A.; Fernandez Perez, M.M.; De La Guardia Cirugeda, M.; Carrion Dominguez, J.L. *Anal. Chem.* **1986,** *58,* 2161.
144. Soroka, K.; Vithanage, R.S.; Phillips, D.A.; Walker, B.; Dasgupta, P.K. *Anal. Chem.* **1987,** *59,* 629.